

June 1985
Vol. 49, No. 1

DEPARTMENT OF
TRANSPORTATION

JUN 11 1985

LIBRARY
PERIODICALS UNIT
M-493.3 0.2

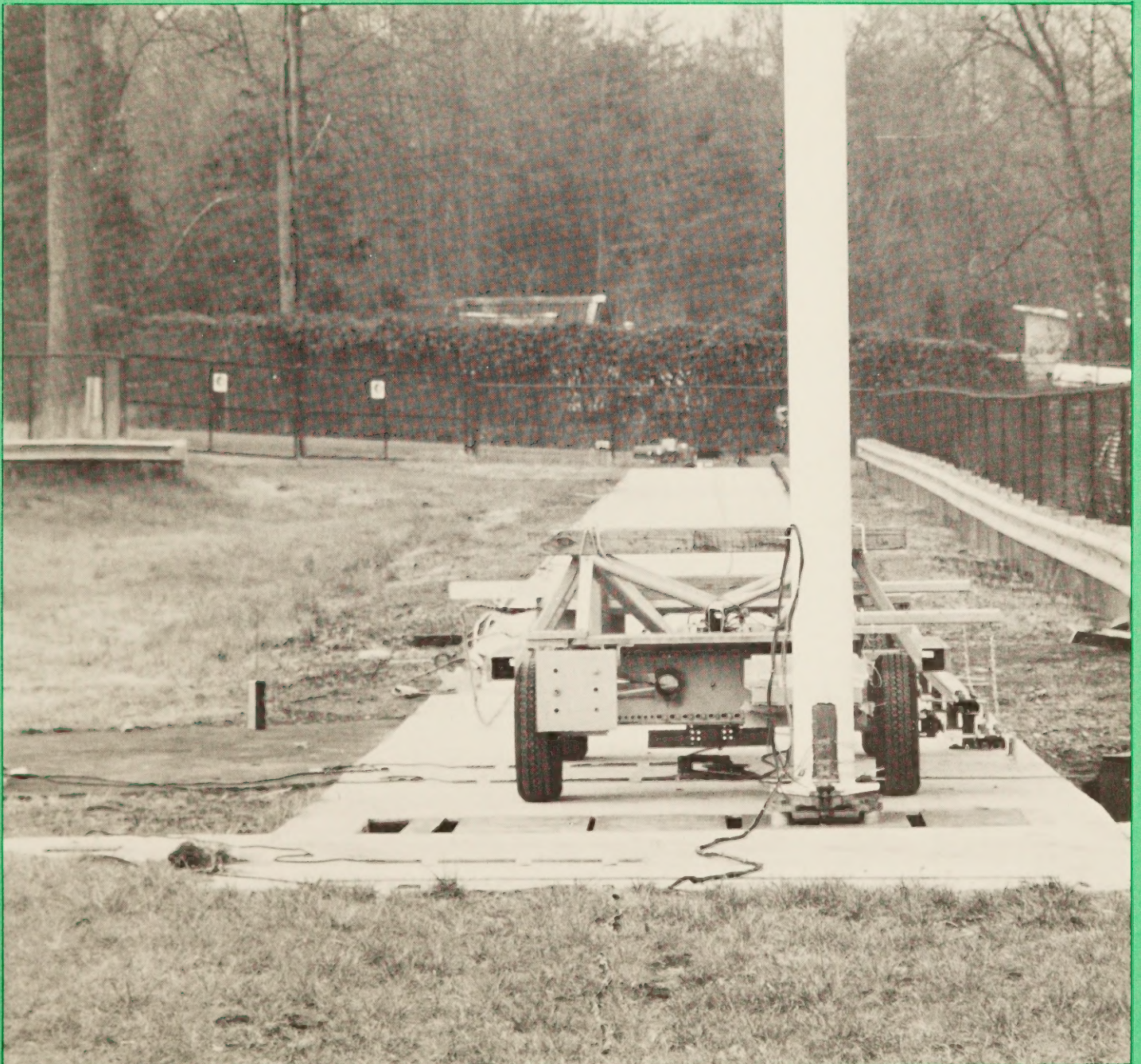


Public Roads

U.S. Department
of Transportation

**Federal Highway
Administration**

A Journal of Highway Research and Development



Public Roads

A Journal of Highway Research and Development

June 1985
Vol. 49, No. 1

U.S. Department of Transportation

Elizabeth Hanford Dole, *Secretary*

Federal Highway Administration

R. A. Barnhart, *Administrator*

U.S. Department of Transportation

Federal Highway Administration
Washington, D.C. 20590

COVER: Impact tests with a bogie vehicle striking breakaway poles are routinely performed at the FOIL, the Federal Outdoor Impact Laboratory, on the grounds of the Turner-Fairbank Highway Research Center in McLean, Virginia.

IN THIS ISSUE

Articles

- The FOIL: A New Outdoor Laboratory for Evaluating Roadside Safety Hardware**
by Martin W. Hargrave 1
- Chemical and Physical Characterization of Binder Materials**
by Brian H. Chollar, John G. Boone, Warren E. Cuff, and Ernest F. Bailey . 7
- Residual Driving Stresses and Vertically Loaded Piles in Cohesionless Soils**
by Jean-Louis Briaud and Albert F. DiMillio 13
- Long Term Monitoring of Pile Foundations**
by Carl D. Ealy and Albert F. DiMillio 18

Public Roads is published quarterly by the Offices of Research, Development, and Technology

David K. Phillips, *Associate Administrator*

Technical Editor

C. F. Scheffey

Editorial Staff

Cynthia C. Ebert

Carol H. Wadsworth

William Zaccagnino

Advisory Board

R. J. Betsold, S. R. Byington, R. E. Hay,

George Shrieves

NOTICE

The United States Government does not endorse products or manufacturers. Trade or manufacturers' names appear herein solely because they are considered essential to the object of the article.

Departments

- Recent Research Reports** 30
- Implementation/User Items** 32
- New Research in Progress** 34

Address changes (send both old and new) and requests for removal for the free mailing list should be directed to:

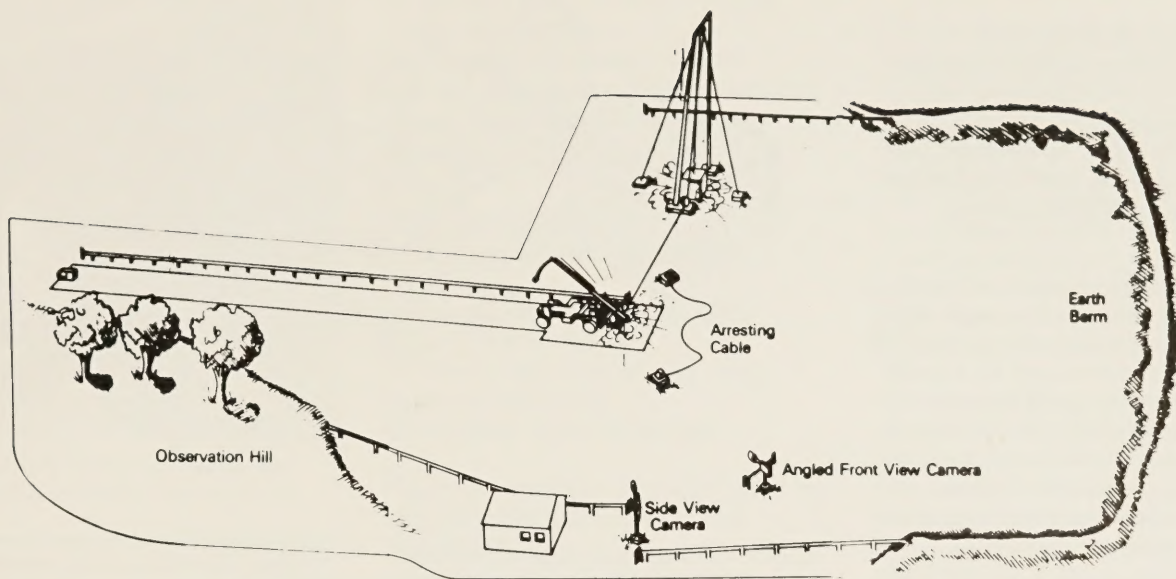
Public Roads Magazine, HRD-10
Federal Highway Administration
6300 Georgetown Pike
McLean, Virginia 22101-2296

At present, there are no vacancies on the FREE mailing list.

Public Roads, A Journal of Highway Research and Development, is sold by the Superintendent of Documents, U.S. Government Printing Office, Washington, D.C. 20402, for \$12 per year (\$3 additional for foreign mailing) or \$3.25 per single copy (81¢ additional for foreign mailing). Subscriptions are available for 1-year periods. Free distribution is limited to public officials actually engaged in planning and constructing highways and to instructors of highway engineering. At present, there are no vacancies on the free mailing list.

The Secretary of Transportation has determined that the publication of this periodical is necessary in the transaction of the public business required by law of this Department. Use of funds for printing this periodical has been approved by the Director of the Office of Management and Budget through May 1, 1990.

Contents of this publication may be reprinted. Mention of source is requested.



The FOIL: A New Outdoor Laboratory for Evaluating Roadside Safety Hardware

by
Martin W. Hargrave

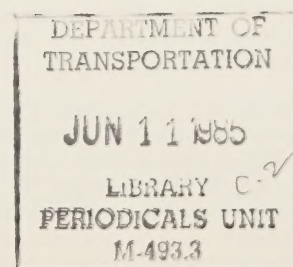
Introduction

Highway safety research to enhance the technology of road building as well as improve the safety of highway users has long been a priority of the Federal Highway Administration (FHWA). Over the years, the FHWA research program has contributed to more efficient, less expensive, and safer roadways.

Much of the federally funded highway research is directed from FHWA's Turner-Fairbank Highway Research Center (TFHRC), in McLean, Virginia. TFHRC, located on 44 acres (17.8 ha) of Federal land near Washington, D.C., consists of offices, laboratories, and outdoor research facilities. A recent addition to this center is an outdoor test facility named the FOIL—the Federal Outdoor Impact Laboratory.¹ Here, roadside safety hardware such as sign supports, light poles, crash cushions, and roadside barriers can be tested and evaluated.

Traditionally, full-scale crash testing has been the standard for the development and evaluation of roadside safety appurtenances because of its reliable, close duplication of real world collision events. However, to reduce test costs and improve the repeatability of test results, alternate test methods have been developed over the years. The latest in this evolution is the FOIL, which can operate in frontal and side impact modes. The display artwork for this article shows an artist's conception of the FOIL in operation during a frontal test.

¹J. A. Hinch, E. D. Howerter, and R. E. Scofield, "Detailed Design Plan for the Updated FHWA FHRS Impact Test Facility—Revision 1," Federal Highway Administration, HSR-20, Washington, D.C., May 21, 1982. Unpublished interim report.



Features of the FOIL

A unique feature of this test laboratory is the reusable bogie test vehicle (fig. 1).^{2 3 4} Currently, this vehicle is designed for frontal testing of breakaway poles, luminaires, and large sign supports and is configured to represent a 1979 Volkswagen Rabbit.

Another significant feature of this test laboratory is the use of a large falling weight as the propulsion system. This falling weight, connected by a cable to the test vehicle, pulls the vehicle forward accelerating it to test speed. Because gravity is free and ever present, this propulsion method provides a reliable and low-cost drive system for the test laboratory.

Side impact testing is another of the test laboratory's singular features. This capability is important because approximately 25 percent of all single-vehicle fatalities result from side impacts into fixed roadside objects. A conceptual drawing of the side impact test device is shown in figure 2. Scheduled to be fully operational in 1986, this test capability uses actual automobiles as test vehicles (fig. 3). Unlike frontal testing, side impact test specifications, evaluation criteria, and vehicle definition are largely undefined. (1, 2)⁵ Consequently, a reusable side impact bogie is not currently being developed but is feasible and may later be developed.

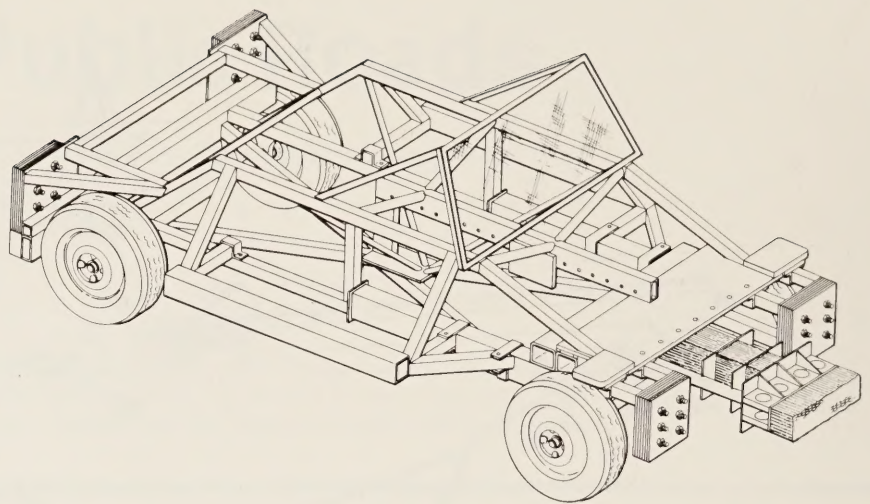


Figure 1. — Frontal impact bogie test vehicle.

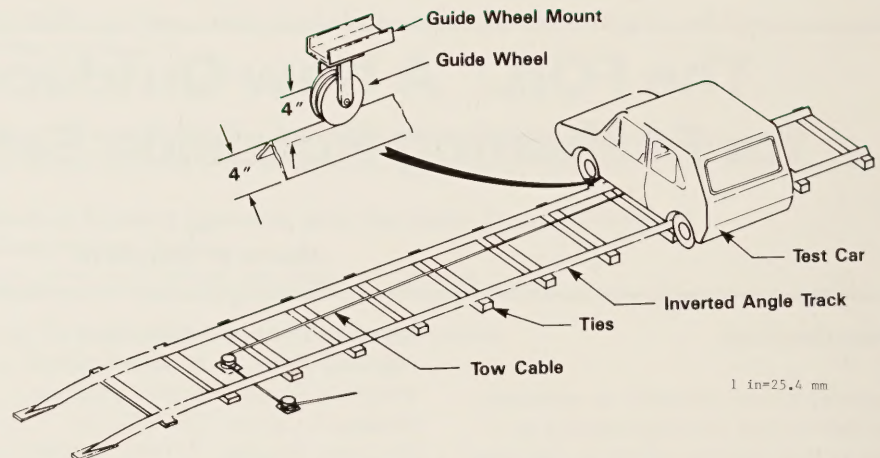


Figure 2. — Conceptual drawing of side impact test device.

Description of the FOIL

The FOIL is located on an irregularly shaped plot of land approximately 400 ft (122 m) long by 200 ft (61 m) at its widest point (see display artwork). This plot contains an approximately 200 ft (61 m) paved acceleration runway followed by a 200 ft (61 m)

by 200 ft (61 m) grassy runout area. The entire site is slightly sloped (2 percent grade) with the highest point located at the head of the runway. The impact area is level for 25 ft (7.6 m) immediately before and 25 ft (7.6 m) following impact with gradual transitions between the sloped runway and the sloped runout area.

²Jeffrey A. Bloom, "Selection of a Vehicle for Frontal and Broadside Impact Testing Into a Luminaire Support—Revised Report," Federal Highway Administration, HSR-20, Washington, D.C., June 1981. Unpublished interim report.

³E. D. Howerter, J. A. Hinch, and R. P. Owings, "Sensitivity Analysis of Subcompact Vehicle Performance Due to an Impact With a Breakaway Luminaire Support—Revision 1, Vols. I and II," Federal Highway Administration, HSR-20, Washington, D.C., Apr. 15, 1983. Unpublished interim report.

⁴J. A. Hinch, P. L. Boyd, and R. P. Owings, "Final Detailed Design Plan for the FHWA TFHRC FOIL Adjustable Bogie, Task C-3," Federal Highway Administration, HSR-20, Washington, D.C., Dec. 1, 1983. Unpublished interim report.

⁵Italic numbers in parentheses identify references on page 6.

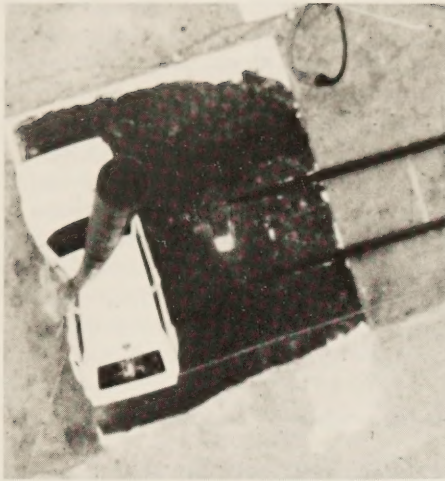


Figure 3.—A 1979 Volkswagen Rabbit side impacting with a breakaway pole at 30 mph (48 km/h).

Acceleration and guidance system

The large weight that powers the FOIL's test vehicle is connected to the front of the vehicle by a cable that is released just before impact. Thus, at impact, the test vehicle is free of all external restraints and is traveling at constant speed. The speed of the vehicle, which varies from 0 to 60 mph (97 km/h) (0 to 45 mph [72 km/h] for side impacts), is determined by the distance of initial pullback. This pullback is accomplished by a winch and second cable attached to the rear of the test vehicle. When the second cable is automatically released, the test sequence is initiated. A single fixed rail and two attachment assemblies fastened to the vehicle's front and rear wheel spindles guide the vehicle. The dual rail system shown in figure 2 guides the vehicle for side impacts.

Because the entire system operates under constant acceleration caused by gravity pulling on the large drop weight, the velocity of the test vehicle at impact can be calculated. The following equation defines the relationship between velocity and pullback distance.⁶

$$V = (2gER \frac{1 + 6S}{1 + R^2W} L)^{1/2}$$

⁶"Monthly Progress Report No. 32 for the Period Oct. 1-28, 1983," EnscO, Inc., contract No. DTFH61-81-C-00036, Federal Highway Administration, HSR-20, Washington, D.C., Nov. 15, 1983, pp. 3-6. Unpublished.

Where,
 V = Impact velocity of test vehicle.
 L = Pullback distance.
 E = System efficiency (75 to 80 percent for frontal impacts—includes losses associated with vehicle).
 W = Weight ratio $\frac{W_V}{W_D}$.

W_V = Vehicle weight.
 W_D = Drop weight (12,500 lb [5.7 Mg]).
 g = Acceleration of gravity (32.2 ft/sec² [9.8 m/sec²]).
 R = Reduction ratio of drop tower pulley system (6:1).
 S = Runway slope (2 percent).

Figure 4, a simple chart developed for operating the FOIL, shows this relationship.⁷

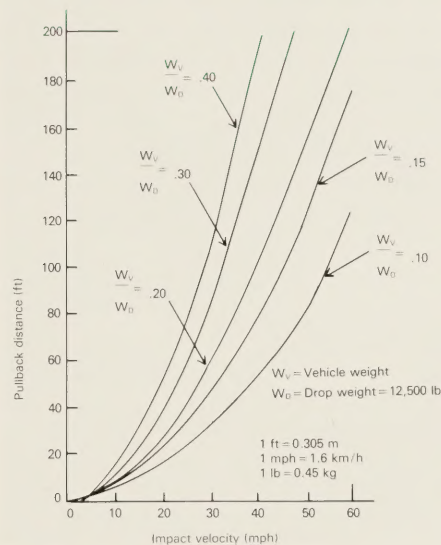


Figure 4.—Pullback distance versus impact velocity.

⁷"FOIL—Pullback Versus Speed Look Up Chart," Dwg. No. 1469-D-2034, EnscO, Inc., contract No. DTFH61-81-C-00036, Federal Highway Administration, HSR-20, Washington, D.C., September 1983.

Test vehicle

The maximum vehicle weight for the full-speed range is 2,250 lb (1.02 Mg) (2,500 lb [1.13 Mg] for side impact). The size of the falling weight and the corresponding strength requirements of the drop tower dictate this weight limit. Heavier vehicles can be tested but at lower maximum speeds. For example, the present system can test a 3,600 lb (1.63 Mg) vehicle—today's large size automobile—at speeds up to 50 mph (80 km/h).

The reusable bogie vehicle (fig. 1) is designed to emulate the actual impact and post-impact performance (the runout) of full-scale automobiles under real world conditions. Any automobile weighing from 1,400 lb (0.64 Mg) to 2,250 lb (1.02 Mg) can be modeled by the bogie.

A principal feature of the FOIL, unlike earlier systems with reusable test devices, is the capability to observe and monitor the runout performance of the bogie after impact. Thus, in addition to analyzing injury severity criteria at impact (1, 2), the tendency for a bogie to rollover after impact also can be observed and analyzed. This capability is important considering the greater likelihood of accident-related rollovers with mini-size vehicles and the higher probability of serious or fatal injury in rollover accidents.

To emulate the crash performance of an actual automobile, computer simulation runs using the Highway Vehicle Object Simulation Model⁸ (3) were produced to determine such properties as wheelbase, weight distribution, and suspension parameters required for a full-scale model. This computer simulation was validated comparing the results with an

⁸E. D. Howerter, J. A. Hinch, and R. P. Owings, "Sensitivity Analysis of Subcompact Vehicle Performance Due to an Impact With a Breakaway Luminaire Support—Revision 1, Vols. I and II," Federal Highway Administration, HSR-20, Washington, D.C., Apr. 15, 1983. Unpublished interim report.

earlier full-scale crash test.⁹ Table 1 lists the properties of the bogie selected. The properties are compared with those of an actual automobile and with those of two earlier test devices, the pendulum and a low speed bogie. (4, 5)

Table 1 shows that the bogie vehicle contains all of the significant properties of an actual automobile except for a suspension system and steerable front wheels. Computer simulation indicates that this vehicle duplicates actual impact and post-impact performance up to 22 ft (6.7 m) following impact and realistically simulates runout trajectory within the remainder of the distance available (22 to 150 ft [6.7 to 45.7 m]). This result is expected because suspension system responses delay impulsive force inputs, and steering systems tend to self-correct with respect to trajectory. Therefore, the lack of steerable front wheels makes the

bogie a worst-case test vehicle regarding rollover. The lack of both steering and suspension also makes the test device rugged and lowers its initial and operating costs.

Arrestor systems

To stop the bogie after impact and runout, three arresting techniques are available—onboard four-wheel braking, an auxiliary energy-absorbing arrestor system, and as a fail-safe, the large earthen berm shown in the display artwork. The onboard braking system is basically a pneumatic-over-hydraulic system; under remote control, air, which is released from an onboard reservoir, acts through a piston at the interface to activate the hydraulic brakes. This braking technique is adequate for test speeds below 40 mph (64 km/h) and without assistance can safely stop the test vehicle after runout. (Braking begins when the vehicle is approximately 50 ft [15.2 m] from the berm.)

the runout area. When the onrushing bogie is snagged by the fence, the kinetic energy of the vehicle is converted to strain energy as the vehicle pulls the metal tapes through and out of the metal bender units.

Finally, as a backup a large earthen berm surrounds the entire runout area. The berm, approximately 6 ft (1.8 m) high with a sand face sloping upward at about 45°, effectively contains out-of-control vehicles.

Data collection systems

The test vehicle can be instrumented with three accelerometers to measure the longitudinal, lateral, and vertical acceleration and three rate gyros to measure the roll, pitch, and yaw angular velocities. All six of these devices are located at the center of gravity of the vehicle and can be used to determine the following occupant injury measures: (1, 2)

- The velocity change of an occupant striking the interior of the vehicle at impact.
- The momentum change of the vehicle such as occurs during a sudden impulsive impact with break-away poles or large sign supports.
- The peak accelerations in the three coordinate directions averaged over 10 or 50 ms.

Two contact switches a fixed distance apart in the runway measure the speed of the test vehicle immediately before impact. The vehicle speed is calculated by measuring the time between successive pulses with a separate timing signal.

Currently, the FOIL data collection system is limited to ten channels of data (nine data signals plus a timing signal), seven of which can be stored on analog magnetic tape for subsequent automatic processing. A high-frequency response strip chart recorder captures data channels in excess of seven, but these additional channels must be manually processed.

In addition to electronic data, film data also are recorded by real time and high-speed 16 mm cameras. Typically, two high-speed cameras

Table 1.—Vehicular properties modeled by various test devices

General category	Specific property	Pendulum	Low-speed bogie	FOIL bogie	Automobile
Crush force/deflection	Centered impacts	X	X	X	X
	Off-center impacts			X	X
Weight properties	Total weight	X	X	X	X
	c.g. location			X	X
	Moments of inertia			X	X
	Products of inertia				X
Geometry	Wheelbase			X	X
	Track width			X	X
	Lower snag simulation	X	X	X	X
	Roof line penetration simulation		X	X	X
Suspension system	Tire stiffness		X	X	X
	Suspension stiffness/damping				X
Steering system	Steerable front wheels				X
Speed capability	0 to 20 mph	X	X	X	X
	0 to 60 mph			X	X

1 mph = 1.6 km/h

At test speeds 40 mph (64 km/h) and above, additional energy-absorbing devices are required. The devices currently in use at the FOIL are two metal bender units that absorb energy by forcing metal tape through a series of staggered rollers. The metal bender units attach to each end of a drag fence that is stretched across

⁹E. D. Howerter, J. A. Hinch, and R. P. Owings, "High Speed Off-Center Frontal Impact of a Minicompact Sedan and a Validated Surrogate Breakaway Luminaire Support—Test Results Report," Test No. 1469 2A82, Ensco, Inc., contract No. DTFH61-81-C-00036, Federal Highway Administration, Washington, D.C., Mar. 12, 1982. Unpublished report.

record the impact (side views) and an additional one records the runout trajectory of the vehicle. Another real time, hand-held camera often is used to record the entire test sequence.

Other equipment

Two additional major pieces of equipment available at the FOIL include a rigid instrumented pole (fig. 5) and an inertia measuring device (IMD) (fig. 6). The crush force of a vehicle's front or side structure is measured by crash testing actual vehicles into the rigid pole. The resulting force data coupled with the corresponding crush distance are required for modeling the bogie vehicle or for computer simulation. In the frontal mode, a single pole segment and two force measuring cells measure the overall crush force of the vehicle's front end. In the side impact mode, however, three pole segments (each with two load cells attached) are used because of the differing stiffness of the door, the roof line, and the lower sill. By using two load cells per segment, the rigid instrumented pole can measure the magnitude as well as the location of the crush force—necessary parameters for modeling.

The IMD determines the rotary moments of inertia or weight distribution of an actual small vehicle, its center of gravity (c.g.), and confirms that these parameters have been replicated in the bogie vehicle. The IMD is basically a simple pendulum or seesaw device on which a vehicle can be placed. The inertia about each axis can be calculated by accurately measuring the period of each oscillation. To measure the vertical c.g., the IMD is tilted through a known angle until it rests on a load cell. The vehicle's vertical c.g. distance can be calculated by accurately measuring the force at the load cell.

Future Plans

Currently, the reusable bogie is designed for frontal impact testing into poles and pole-like objects, and the next logical step in its development is to provide a full-width frontal crush capability. This technically possible capability would allow crash cushions and similar roadside objects to be tested.



Figure 5. — Rigid instrumented pole.

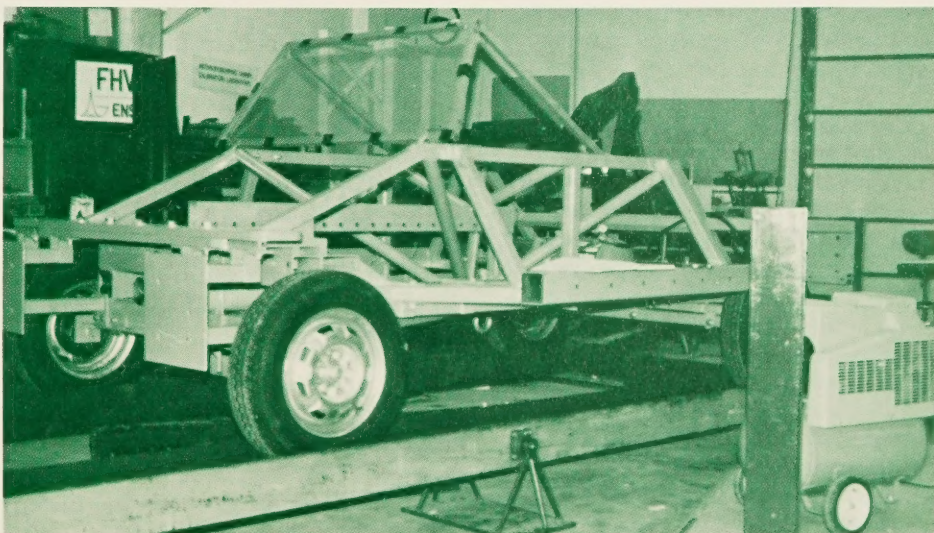
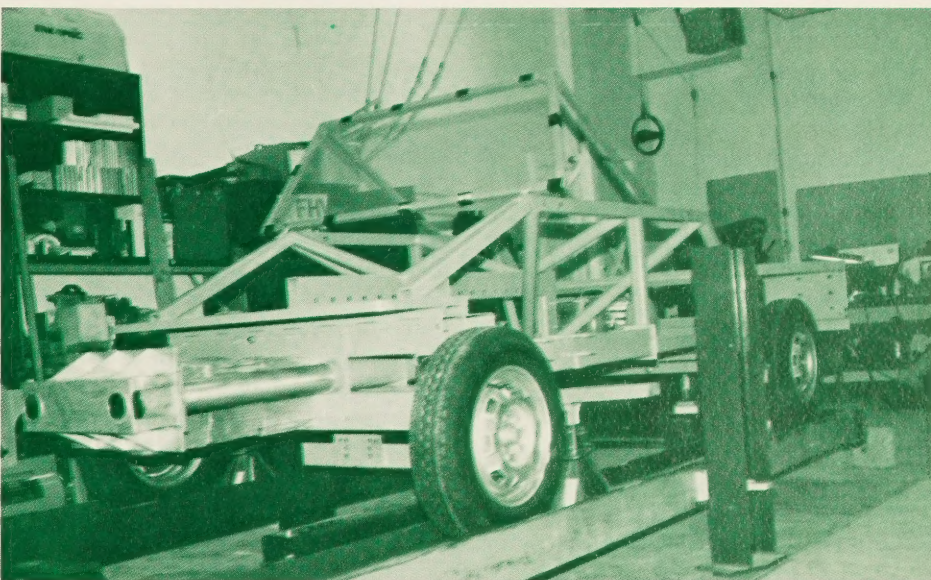


Figure 6. — Inertia measuring device.

A second step is the development of a two-dimensional (longitudinal and lateral) crush bogie capable of testing roadside barriers. However, in addition to the complexity of a two-dimensional crush cartridge, a bogie capable of testing barriers would most likely require a complete suspension system and steerable front wheels for proper modeling. Although a two-dimensional crush vehicle is technically feasible, it may be too expensive and not rugged enough for the FOIL, making the practicality of such a vehicle uncertain.

Other improvements include an expansion of the data collection and processing system. This system currently has the capability to record in analog form seven channels of data (six channels of data plus one timing signal) for subsequent automatic processing. An increase to a maximum of 44 channels is contemplated. An upgrade of this system is planned to significantly increase this system's capability and allow the following data to be collected and processed:

- Anthropomorphic dummy data from frontal or side impact dummies (8 to 16 channels frontal, 18 to 36 channels side impact).
- Crush force of a vehicle's front or side structure measured with a rigid instrumented pole (2 channels frontal, 6 channels side impact).
- Additional vehicle and test article instrumentation to determine specific parameters of interest during a test series (0 to 6 channels).

A microcomputer and a digitizer also will be added to process these data and provide numerical and graphical output. The digitizer converts the data from an analog to a digital form so the microcomputer can process it. These enhanced processing and data collection capabilities make the FOIL a self-contained system capable of rapid analysis and accurate results.

In addition to the improvements just described, a pole and luminaire testing program is envisioned to update our knowledge of current

breakaway poles and signs as well as to provide information on the potential for occupant injury from mini-vehicle collisions with currently approved breakaway hardware. Testing in both the frontal and side impact modes is planned. Side impact testing, unlike frontal or head-on testing, has received little attention from the highway research community. Not only must various kinds of breakaway hardware be tested to determine acceptability under dynamic side impact test conditions, but the test conditions, evaluation criteria, and test vehicle must also be defined for the upcoming test program.

It is anticipated that States and other organizations will initiate test programs for the FOIL using the bogie test vehicle. Test programs that can be performed by other research organizations and which create a situation of competition (for example, full-scale crash testing and FHWA pendulum testing) are not eligible for the FOIL. For acceptable programs, all test activities will be performed by the FOIL support and maintenance contractor in accordance with established operating and safety procedures; users may participate during actual testing only as observers. A schedule of charges for testing services has been compiled and is available from the FOIL manager, Federal Highway Administration, HSR-20, Turner-Fairbank Highway Research Center, 6300 Georgetown Pike, McLean, Virginia 22101-2296.

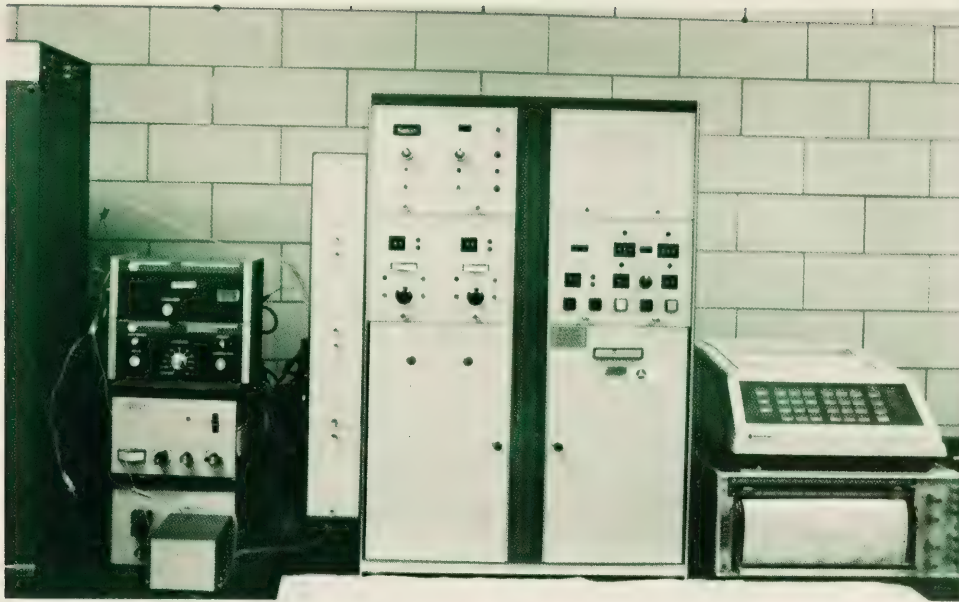
The FOIL is a modern test facility designed and constructed to solve many of the roadside safety problems of the 1980's and beyond. As primarily a small car crash test facility, it will be used to research the higher probability of injury for small-car occupants. As a side impact test facility, it will be used to develop side impact technology and appropriate roadside solutions.

The FOIL—the Federal Outdoor Impact Laboratory is a new outdoor laboratory for evaluating roadside safety hardware and is one more step in the development of a safer highway environment for our Nation's motoring public.

REFERENCES

- (1) "Recommended Procedures for Vehicle Crash Testing of Highway Appurtenances," Transportation Research Circular No. 191, *Transportation Research Board, National Academy of Sciences*, Washington, D.C., February 1978.
- (2) Jarvis D. Michie, "Recommended Procedures for the Safety Performance Evaluation of Highway Appurtenances," National Cooperative Highway Research Program Report No. 230, *Transportation Research Board, National Academy of Sciences*, Washington, D.C., March 1981.
- (3) David J. Segal, "Highway Vehicle Object Simulation Model—Vols. I-IV," Report Nos. FHWA-RD-76-164/165, *Federal Highway Administration*, Washington, D.C., February 1976.
- (4) D. B. Chisholm and L. C. Meczkowski, "Dynamic Testing of Luminaire Supports With an Improved Pendulum Impact Facility," Report No. FHWA-RD-78-204, *Federal Highway Administration*, Washington, D.C., September 1978.
- (5) J. A. Bloom and J. A. Hinch, "Laboratory Evaluation of Existing Breakaway Structures—Vols. I and II," Report Nos. FHWA-RD-79-139/140, *Federal Highway Administration*, Washington, D.C., June 1980.

Martin W. Hargrave is a mechanical research engineer in the Safety Design Division, Office of Safety and Traffic Operations R&D, FHWA. He currently is manager of the FOIL and also manages contract research in several areas of highway safety, including roadside safety hardware and large truck safety. He actively participates on two ongoing NCHRP project panels dealing with roadside safety hardware issues. Before joining FHWA in 1979, Mr. Hargrave's career encompassed 17 years of varied engineering assignments with several companies including Control Data Corporation and NCR Corporation.



Chemical and Physical Characterization of Binder Materials

by
Brian H. Chollar, John G. Boone, Warren E. Cuff, and Ernest F. Bailey

Introduction

Researchers at Montana State University developed a high-pressure gel permeation chromatography (HPGPC) technique for separating the components in asphalt cement according to their molecular size. (1)¹ A model asphalt with a certain large molecular size (LMS) composition has been proposed for each State based on asphalt tests from pavements in 15 States. (2) The researchers theorized that a direct relationship exists between the amount of LMS material in an asphalt and the thermal cracking properties of pavements incorporating that asphalt. (3) However, paving mix design, construction practices, climatological conditions, and traffic type and volume have to be considered before unequivocal relationships between asphaltic composition and pavement performance can be shown.

For this HPGPC method to be a valid tool for predicting pavement performance, a good correlation is required between HPGPC properties of asphalts and those physical properties related to stiffness. In a study of the relationship between the limiting stiffness temperature (LST) of asphalts calculated from penetrations measured at three different temperatures versus thermal cracking of

pavements that incorporated these asphalts, it was found that low-temperature asphalt and asphalt-aggregate mixture stiffnesses, of which the LST is a reasonable measure, correlate well with pavement transverse cracking. (4)

This article addresses this correlation by determining the HPGPC characteristics of a group of asphalts and relating these characteristics to the physical properties of asphalts.

Background

Studying correlations of the long-term performance of asphaltic pavements with various asphalt physical properties led to the development of asphalt specifications that contain limits on properties such as penetration and viscosity. Currently, asphalt specifications assure that the asphalt will act in a predictable manner during handling and construction and will meet minimum quality levels.

In the last 10 years, however, concern has arisen that although asphalt meets specifications, it lacks the quality once routinely obtained. Specifically, current asphalt products are not providing the long service life once achieved. As a result, many studies have been initiated to find better ways to characterize asphalts and to relate their composition, rheology, and physical properties to asphaltic pavement performance. Much of this research is

¹Italic numbers in parentheses identify references on page 12.

centered on the thermal cracking behavior of asphaltic pavements. Following is an excellent, succinct description of the mechanism of thermal cracking:

"Since an asphalt concrete road-slab is completely restricted in length any shrinkage or expansion due to changes in temperature have to be accommodated by the asphalt concrete. During the warm season, the amount of viscous flow per unit time can be very large and the pavement surface easily accommodates the expansion from warming and constriction from cooling. However, during the winter as temperatures drop, the ability of the asphalt to flow lessens, and if temperatures drop rapidly, the shrinkage rate can exceed the accommodation by viscous flow. Tensile stresses develop in asphalt concrete and cracking occurs when the tensile stresses or strains exceed the limit of the asphalt concrete; the cracking will be transverse in nature." (5)

Based on this description, thermal cracking is caused by rapid changes in temperature and not by low temperatures. ("Rapid" is not defined.) Consequently, it is easier to design an asphaltic pavement that performs without cracking in a constant temperature range of -40 to -60°F (-40 to -51°C) than in a temperature that fluctuates overnight from 45 to 0°F (7.2 to -18°C).

Much of the predictive treatment of thermal cracking is concerned with the concept of stiffness. The stiffness of a material (S) is a modulus relating its tensile stress (σ) to its tensile strain (ϵ). Because of the viscoelastic behavior of asphalt materials, the stiffness modulus of asphalts is time and temperature dependent, that is,

$$S(t, T) = \sigma / \epsilon(t, T)$$

For a particular asphalt, the temperature range over which it exhibits elasticity is critical in assessing its behavior at low service temperatures.

Obviously, the stiffness of the asphalt component strongly determines the stiffness of an asphalt-aggregate mixture. However, research indicates that other factors such as the air void content and the aggregate gradation have a significant but lesser influence. (5, 6)

The stiffness of an asphalt or asphalt-aggregate mixture has been measured in various ways. One method estimates the stiffness with nomographs. The nomographs are entered by use of the penetration index (PI), a measure of the change in penetration with temperature. (6) Another method advocates using the pen viscosity number (PVN) instead of the PI. (7) The indirect tensile test was used to determine the stiffness modulus for a series of six AC-20 asphalts used in Pennsylvania. Results indicate a variation in stiffness is possible in a single grade of asphalt. (8) Predicting low-temperature behavior by measuring fundamental asphalt properties such as viscosity in the desired temperature range also has been evaluated. (9-11)

Researchers at Texas A&M University have used fracture mechanics to measure the fracture toughness by evaluating the surface integral J_{Ic} used to characterize the local stress-strain field for a two-dimensional crack. (12, 13) This method applies to elastic-plastic fracture phenomena and is particularly suited to evaluating low-temperature performance below the glass transition temperature of the material. In addition, the low-temperature behavior of sulfur-based binders has been studied with this method, which can discriminate among several binders with similar chemical makeup. This method goes beyond simple predictive procedures based on stiffness and other factors in that it provides a measure of the energy needed to drive crack formation. Within test limits, this method can determine the relationship between crack growth energy and temperature.

Experimental Approach

A study was initiated to measure the HPGPC properties of asphalt under the same conditions as used in the Montana State University study and to compare the LMS results with the selected properties of the asphalts.

HPGPC involves the separation of asphaltic materials into their components according to molecular size (fig. 1). The asphalt sample is introduced into a liquid flowing at high pressure through a column packed with a highly porous, solid material. The liquid transports the asphalt through and around the porous packing material in the column and as a result:

"Smaller size molecules in the asphalt can enter freely into all the pores of the column packing while very large molecules can enter none of those pores. Molecules of intermediate size have access to varying amounts of available pore volume. Therefore, the larger molecules move through the column more rapidly than the smaller ones." (14)

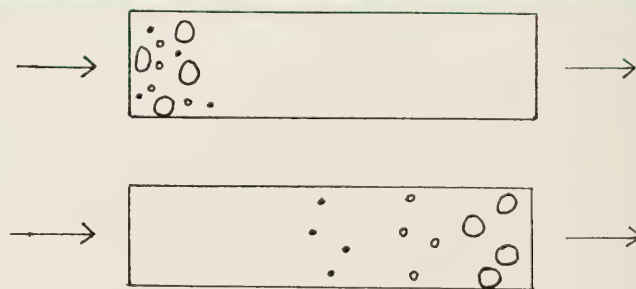


Figure 1. Size separation of asphalts.

The LMS portion of the asphalt leaves the column, followed by the medium-size and then the small-size components. A detector measures the amount of each component, and the percent of LMS material of the asphalt is calculated.

Basically these procedures are the same as those used in the Montana State University studies. A series of ten asphalts were analyzed using HPGPC, and the LMS of these asphalts was determined using four different data slice combinations of the chromatograms. Next, five asphalts from the Montana State University study were analyzed, and the LMS content was calculated and compared with the Montana State University values to make sure the values agreed. The LMS content of another series of 28 asphalts was then determined by this method, and the correlations between the LMS content and seven physical properties of the asphalts were calculated.

Materials, Equipment, and Instrumentation

Five new μ -styragel columns, an ultraviolet detector operating at 340 $m\mu$, and an eluent flow rate of 2 ml/min (table 1) were used to separate these asphalts. Tetrahydrofuran (THF) was used both as a solvent for the asphalts and as an eluent for HPGPC. Refluxing this solvent with sodium metal and benzophenone until a lavender color persisted dried it further; next, it was distilled under dry nitrogen gas and kept in a nitrogen atmosphere until used, usually within 24 hours. This drying procedure is one of the most important steps in the separation process because percentages of LMS in asphalt will decrease substantially when traces of water are present in the THF eluent. Percentages of water in the distilled THF were determined by infrared spectroscopy by comparing the spectrum of each distilled material with reference spectra of THF solutions containing varying amounts of water. THF containing 0.02 to 0.04 percent H_2O was used in the asphalt HPGPC analyses.

Table 1.—Conditions used for the high-pressure gel permeation chromatography of asphalts

Columns:	5 μ -styragel columns arranged in the order: 3-500 A [®] 1-1000A [®] 1-100A [®]
Solvent:	Dry Tetrahydrofuran
Detector:	Ultraviolet and visible wavelength spectrophotometric detector at 340 $m\mu$
Sample:	Solution of 2 percent asphalt
Reference:	0.5 percent polystyrene, measured at 254 $m\mu$
Elution Rate:	2 ml/min

A detector wavelength of 254 $m\mu$ was used in the early asphalt HPGPC studies at Montana State University. Recently, however, the detector wavelength was increased to 340 $m\mu$ to make the LMS measurements more precise.

In addition, Montana State University has begun using ultra- μ -styragel columns for the asphalt analyses instead of the μ -styragel columns used in their earlier work. In this study the μ -styragel columns with the same pore diameter were used. No difference exists in the analytical data obtained from either kind of column, but analysis is a little faster using the ultra- μ -styragel columns.

A Spectra Physics 3500 Research High Pressure Liquid Chromatograph, a Spectra Physics 770 Spectroflow variable wavelength ultraviolet detector, and a Spectra Physics SP4270 Computing Integrator were used in this study.

Calculations

Data slices

The SP4270 Computing Integrator automatically prints the chromatogram of each asphalt after each run, divides the area of the chromatogram into data slices by timed increments (fig. 2), and computes the area percentage for each slice of the total curve. The time per slice was set at 1/3 minute. The time to obtain a chromatogram for a single asphalt was 30 minutes. The data collection for each slice was started 10 minutes after injection. The total number of data slices was 60.

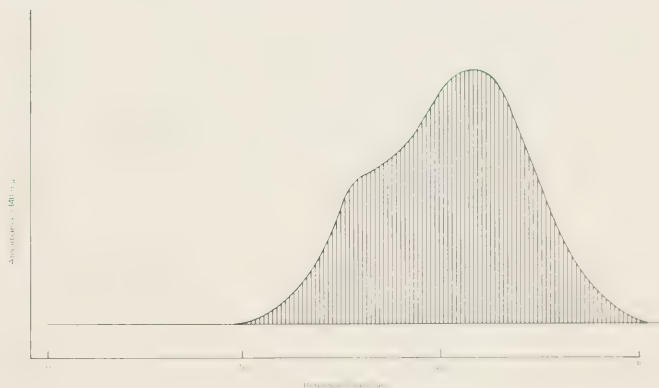


Figure 2. — High-pressure gel permeation chromatographic separation of asphalts.

Slices containing LMS content

A series of eleven asphalts used in an asphalt fingerprinting study were subjected to the HPGPC analysis. (15) The LMS percentage of each asphalt was calculated by totaling the data from the first 18, 19, 20, and 22 data slices of each chromatogram and calculating the percentage of the total of all 60 data slices for that chromatogram (table 2). The various "slice fractions" (18/60, 20/60, etc.) were found to give the same result when judged by the t-test (1 percent significance level); the 19/60 ratio was used in subsequent tests.

Table 2.—LMS of asphalt samples for differing data slices

Asphalt laboratory No.	Percentage LMS			
	18 60 ¹	19 60	20 60	22 60
C-7660	7.0	9.9	13.4	25.3
C-7831	2.0	3.6	5.9	17.6
C-8036	4.4	6.9	10.0	18.2
C-8265	5.7	8.5	12.1	21.2
C-8271	6.8	9.4	12.5	20.2
C-7815	8.0	11.2	14.9	23.6
C-7891	6.3	9.1	12.5	20.9
C-7559	1.6	2.9	4.9	11.1
C-8089	5.5	8.2	11.6	20.2
C-7829	1.7	3.1	5.0	11.2
C-7702	4.7	7.1	10.2	18.3

¹Number of data slices for the LMS and the total asphalt content, respectively.

Five asphalts obtained from Montana State University of known LMS content were run using the HPGPC method, and the LMS percentages were calculated for ratios of 20 out of 60 and 19 out of 59 data slices (table 3). T-tests were run between the 19/59 and the Montana State University values and the 20/60 and Montana State University values; neither set differed significantly from the Montana State University data when tested against the appropriate t-value at the 99 percent probability level. Thus, all subsequent LMS percentage calculations were made using 19 out of 59 data slices for LMS content.

Table 3.—LMS of asphalts obtained from Montana State University and the Federal Highway Administration

Montana State University Sample No.	Percentage LMS		
	Montana	FHWA	
		20/60 ¹	19/59
Ohio 23A	38.0	44.6	39.4
Georgia 1A	41.8	37.5	32.6
Colorado 6A	24.6	19.4	15.3
New Jersey 11A	24.0	21.1	16.5
Montana 36C	19.0	8.6	5.9

¹Number of data slices for the LMS and the total asphalt content, respectively.

Experimental Data

Twenty-eight asphalts were analyzed with the HPGPC technique and the LMS contents were calculated. Table 4 shows the LMS percentage and physical data for these asphalts. (16)

A linear regression calculation was made for these data using LMS as the dependent variable and each of the physical data as the independent variable. The calculations of the correlation coefficients (R^2) were conducted using a procedure (17) for R^2 with the Mallow's CP option, which is a measure of the influence the independent variables have on the dependent variable. (18) This option uses the mean squared error and other relevant statistics to estimate the number of variables necessary to produce the best model for the equation:

$$y = \alpha + \beta X_1 + \beta_2 X_2 + \dots + \beta_n X_n$$

Where,

$\alpha, \beta_1, \beta_2, \dots, \beta_n$ = constants.

y = LMS content.

X_1, X_2, \dots, X_n = the physical properties of asphalt significant to the relation with LMS.

The best model is based on the combination of asphalt property variables giving the lowest CP.

Multivariate analysis also was used to calculate the probability that certain variables do not significantly influence the prediction of LMS. (19)

TABLE 4. CHROMATOGRAPHY DATA AND PHYSICAL PROPERTIES OF ASPHALT SAMPLES

LAB NUMBER	LMS	DUCT45	DUCT77	SG	SHR SUS	ASPH	REF IND	LST
B2908	32.23	31	130	1.004	0.36	19.0	1.4827	-46
B2909	32.15	9	221	1.007	0.39	20.5	1.4826	-45
B2910	27.01	9	200	1.012	0.51	21.6	1.4817	-41
B2921	12.70	8	250	1.004	0.42	15.5	1.4837	-39
B2922	9.43	0	250	1.007	0.62	18.1	1.4844	-39
B2960	23.96	11	160	1.034	0.42	27.9	1.4775	-51
B2962	17.75	150	155	1.010	0.21	19.3	1.4815	-51
B2963	17.24	150	250	1.015	0.31	20.2	1.4819	-48
B2964	15.98	10	241	1.021	0.44	21.6	1.4822	-44
B2975	8.79	0	215	1.005	0.66	16.5	1.4851	-20
B3009	15.57	12	230	0.994	0.41	17.8	1.4833	-50
B3010	23.07	7	205	0.995	0.49	20.1	1.4813	-54
B3013	26.88	150	245	1.021	0.32	20.8	1.4810	-39
B3014	14.58	14	250	1.025	0.39	21.6	1.4814	-42
B3028	16.09	3	152	1.011	0.30	19.5	1.4806	-53
B3030	12.40	5	250	1.028	0.59	29.3	1.4812	-41
B3036	12.64	11	210	1.026	0.42	16.7	1.4827	-56
B3051	16.13	150	250	1.028	0.18	26.1	1.4769	-46
B3056	11.52	3	250	1.020	0.64	19.2	1.4806	-34
B3058	22.61	150	140	1.021	0.31	22.4	1.4790	-46
B3108	16.27	244	167	1.011	0.23	17.3	1.4851	-40
B3109	18.43	19	250	1.014	0.43	18.6	1.4850	-33
B3110	14.93	9	250	1.018	0.54	19.7	1.4821	-36
B3578	14.11	150	205	1.015	0.21	18.1	1.4890	-35
B3579	11.66	150	245	1.010	0.40	18.0	1.4897	-35
B3601	6.96	250	171	1.011	0.29	9.7	1.4863	-30
B3602	16.50	12	250	1.016	0.50	11.0	1.4867	-23
B3603	3.47	4	250	1.021	0.65	12.2	1.4868	-22

LMS = Large Molecular Size Content (%)
 DUCT = Ductility at 45°F and 77°F
 SG = Specific Gravity
 SHR SUS = Shear Susceptibility
 ASPH = Asphaltene Content (%)
 REF IND = Refractive Index
 LST = Limiting Stiffness Temperature (°C)

¹F = 1.8°C + 32

Results

Table 5 gives the R^2 and Mallows' CP values for various combinations of asphalt physical variables. The combination of asphaltenes, specific gravity, and ductility at 77°F (25°C) gives the best model with the lowest CP and an R^2 value of 0.386. The equation describing this model is:

$$\text{LMS} = 2.355 - 0.000565 \text{ DUCT } 77 - 2.203 \text{ SG} + 0.8817 \text{ ASPH}$$

Multivariate analysis of this model shows the following probabilities that the variables do not influence LMS:

- DUCT 77—5.60 percent.
- SG—10.80 percent.
- ASPH—0.59 percent.

This study shows that for single relationships LST correlates best with LMS of the 7 parameters studied.

However, this relationship has an R^2 value of 0.230, meaning that differences among the LST values of the asphalts explain only 23 percent of the variation in LMS values.

The best relationship of the parameters studied to LMS content is the combination of asphaltenes, specific gravity, and ductility at 77°F (25°C). Because the R^2 value for this relationship is 0.386, only 39 percent of the variation of the LMS among the 28 asphalts can be explained by corresponding variations in the three independent variables.

Conclusions and Recommendations

This study addresses the relationship of asphaltic HPGPC characteristics to the major physical properties used for the specification of asphalts and for the prediction of the performance of pavements containing the asphalts. Results of this study indicate that the LMS content of the asphalts has only a minor influence on the physical properties examined. Therefore, other effects not identified play an important role in the variation of LMS among asphalts.

More research is needed to define the relationship between the LMS content of an asphalt and its physico-chemical properties. Perhaps combinations of these properties in combination with asphalt physical characteristics will provide a stronger correlation with the LMS content of asphalts. It is significant, however, that there is little correlation between the LMS of the asphalts and their LST values for the 28 asphalts studied. This indicates that extreme caution is warranted when considering HPGPC as a tool for predicting the potential low-temperature behavior of any particular asphalt.

TABLE 5. REGRESSION MODELS FOR DEPENDENT VARIABLE LMS

NUMBER IN MODEL	R-SQUARE	CP(1)	VARIABLES IN MODEL
1	0.002	14.36	DUCT45
1	0.011	14.00	SG
1	0.097	10.49	SHR SUS
1	0.150	8.66	DUCT77
1	0.175	7.68	ASPH
1	0.186	7.26	REF IND
1	0.229	5.60	LST

2	0.012	15.94	DUCT45 SG
2	0.111	12.16	SG SHR SUS
2	0.153	10.55	DUCT77 SG
2	0.174	9.74	DUCT77 SHR SUS
2	0.175	9.68	DUCT45 ASPH
2	0.179	9.52	DUCT45 DUCT77
2	0.187	9.25	DUCT45 REF IND
2	0.211	8.32	ASPH REF IND
2	0.231	7.54	DUCT45 LST
2	0.240	7.20	SG LST
2	0.241	7.15	SHR SUS LST
2	0.249	6.84	SHR SUS ASPH
2	0.253	6.70	DUCT45 SHR SUS
2	0.253	6.67	SHR SUS REF IND
2	0.259	6.45	REF IND LST
2	0.267	6.17	ASPH LST
2	0.271	6.00	SG REF IND
2	0.278	5.74	DUCT77 LST
2	0.282	5.56	DUCT77 REF IND
2	0.283	5.55	SG ASPH
2	0.286	5.33	DUCT77 ASPH

3	0.179	11.55	DUCT77 SG SHR SUS
3	0.181	11.47	DUCT45 DUCT77 SG
3	0.212	10.29	DUCT45 ASPH REF IND
3	0.241	9.15	DUCT45 SG LST
3	0.252	8.71	SG SHR SUS LST
3	0.259	8.44	DUCT45 REF IND LST
3	0.264	8.29	DUCT45 SG SHR SUS
3	0.267	8.17	DUCT45 ASPH LST
3	0.272	7.96	ASPH REF IND LST
3	0.275	7.86	DUCT45 SG REF IND
3	0.277	7.77	SHR SUS ASPH REF IND
3	0.279	7.68	DUCT77 SHR SUS LST
3	0.281	7.60	SHR SUS REF IND LST
3	0.283	7.54	DUCT77 SG LST
3	0.285	7.45	DUCT45 SG ASPH
3	0.288	7.34	SHR SUS ASPH LST
3	0.290	7.28	DUCT45 DUCT77 REF IND
3	0.291	7.25	DUCT45 SHR SUS LST
3	0.292	7.18	DUCT45 DUCT77 LST
3	0.301	6.83	DUCT77 SHR SUS REF IND

3	0.305	6.69	SG REF IND LST
3	0.313	6.39	DUCT77 REF IND LST
3	0.322	6.02	DUCT45 DUCT77 SHR SUS
3	0.325	5.99	DUCT45 SHR SUS REF IND
3	0.325	5.94	DUCT77 ASPH REF IND
3	0.325	5.91	SG ASPH LST
3	0.327	5.86	DUCT45 DUCT77 ASPH
3	0.328	5.80	DUCT77 SHR SUS ASPH
3	0.330	5.72	SG ASPH REF IND
3	0.333	5.63	DUCT77 SG REF IND
3	0.333	5.60	DUCT45 SHR SUS ASPH
3	0.336	5.52	SG SHR SUS REF IND
3	0.339	5.39	DUCT77 ASPH LST
3	0.354	4.80	SG SHR SUS ASPH
3	0.386	5.59	DUCT77 SG ASPH

4	0.272	9.96	DUCT45 ASPH REF IND LST
4	0.285	9.47	DUCT77 SG SHR SUS LST
4	0.296	9.05	DUCT45 DUCT77 SG LST
4	0.297	9.00	SHR SUS ASPH REF IND LST
4	0.301	8.85	DUCT45 SG SHR SUS LST
4	0.306	8.65	DUCT45 SG REF IND LST
4	0.319	8.17	DUCT77 SHR SUS REF IND LST
4	0.320	8.11	DUCT45 DUCT77 REF IND LST
4	0.326	7.89	DUCT45 DUCT77 SG SHR SUS
4	0.326	7.88	DUCT45 SG ASPH LST
4	0.327	7.86	DUCT45 SHR SUS REF IND LST
4	0.333	7.61	DUCT45 DUCT77 ASPH REF IND
4	0.334	7.57	DUCT45 DUCT77 SG REF IND
4	0.336	7.49	DUCT45 SG ASPH REF IND
4	0.338	7.44	DUCT45 SHR SUS ASPH LST
4	0.339	7.38	DUCT77 SHR SUS ASPH REF IND
4	0.340	7.35	DUCT45 DUCT77 SHR SUS LST
4	0.340	7.35	SG SHR SUS REF IND LST
4	0.342	7.29	DUCT77 ASPH REF IND LST
4	0.343	7.23	DUCT45 SHR SUS ASPH REF IND
4	0.343	7.22	DUCT77 SHR SUS ASPH LST
4	0.345	7.15	SG ASPH REF IND LST
4	0.347	7.09	DUCT77 SG REF IND LST
4	0.349	7.01	DUCT45 DUCT77 ASPH LST
4	0.359	6.84	DUCT77 SG SHR SUS REF IND
4	0.362	6.52	SG SHR SUS ASPH LST
4	0.376	6.02	DUCT45 DUCT77 SHR SUS REF IND
4	0.380	5.83	DUCT45 SG SHR SUS REF IND
4	0.390	5.44	DUCT45 DUCT77 SG ASPH
4	0.3935	5.32	DUCT77 SG ASPH LST
4	0.3935	5.31	SG SHR SUS ASPH REF IND
4	0.4050	4.87	DUCT77 SG SHR SUS ASPH
4	0.4055	4.85	DUCT77 SG ASPH REF IND
4	0.4068	4.80	DUCT45 DUCT77 SHR SUS ASPH
4	0.407	4.75	DUCT45 SG SHR SUS ASPH

5	0.344	9.20	DUCT45 DUCT77 SG SHR SUS LST
5	0.344	9.18	DUCT45 SHR SUS ASPH REF IND LST
5	0.347	9.06	DUCT77 SHR SUS ASPH REF IND LST
5	0.348	9.04	DUCT45 SG ASPH REF IND LST
5	0.349	9.02	DUCT45 DUCT77 SG REF IND LST
5	0.350	8.97	DUCT45 DUCT77 ASPH REF IND LST
5	0.361	8.55	DUCT77 SG SHR SUS REF IND LST
5	0.375	8.02	DUCT45 DUCT77 SHR SUS REF IND LST
5	0.380	7.81	DUCT45 SG SHR SUS REF IND LST
5	0.393	7.51	SG SHR SUS ASPH REF IND LST
5	0.396	7.18	DUCT45 DUCT77 SG ASPH LST
5	0.406	6.82	DUCT77 SG SHR SUS ASPH LST
5	0.406	6.81	DUCT45 DUCT77 SG ASPH REF IND
5	0.406	6.81	DUCT77 SG ASPH REF IND LST
5	0.407	6.79	DUCT45 DUCT77 SHR SUS ASPH LST
5	0.408	6.74	DUCT45 DUCT77 SHR SUS ASPH REF IND
5	0.408	6.74	DUCT45 SG SHR SUS ASPH REF IND LST
5	0.408	6.72	DUCT45 DUCT77 SG SHR SUS REF IND
5	0.426	6.06	DUCT77 SG SHR SUS ASPH REF IND
5	0.427	6.00	DUCT45 SG SHR SUS ASPH REF IND
5	0.458	4.83	DUCT45 DUCT77 SG SHR SUS ASPH

6	0.407	8.76	DUCT45 DUCT77 SG ASPH REF IND LST
6	0.409	8.71	DUCT45 DUCT77 SHR SUS ASPH REF IND LST
6	0.410	8.66	DUCT45 DUCT77 SG SHR SUS REF IND LST
6	0.427	8.02	DUCT77 SG SHR SUS ASPH REF IND LST
6	0.434	7.72	DUCT45 SG SHR SUS ASPH REF IND LST
6	0.444	6.57	DUCT45 DUCT77 SG SHR SUS ASPH LST
6	0.465	6.56	DUCT45 DUCT77 SG SHR SUS ASPH REF IND LST

7	0.479	8.00	DUCT45 DUCT77 SG SHR SUS ASPH REF IND LST

LMS = Large Molecular Size Content (%)
 DUCT = Ductility at 45°F and 77°F (cm/min.)
 SG = Specific Gravity
 SHR SUS = Shear Susceptibility
 ASPH = Asphaltene Content (%)
 REF IND = Reflective Index
 LST = Limiting Stiffness Temperature (°C)

REFERENCES

- (1) P. W. Jennings et al., "Chemical Composition of Commercial Asphalt Cement as Determined by High Pressure Liquid Chromatography," Report No. FHWA MT 7929, *Montana Department of Highways*, 1977.
- (2) P. W. Jennings et al., "The Expanded Montana Asphalt Quality Study Using High Performance Liquid Chromatography," *Montana Department of Highways*, August 1984.
- (3) P. W. Jennings et al., "High Pressure Liquid Chromatography as a Method of Measuring Asphalt Composition," Report No. FHWA MT 7930, *Montana Department of Highways*, 1980.
- (4) "Design Techniques to Minimize Low-Temperature Asphalt Pavement Transverse Cracking," Research Report No. RR 81-1, *The Asphalt Institute*, December 1981.
- (5) H. J. Fromm and W. A. Phang, "A Study of Transverse Cracking of Bituminous Pavements," Vol. 41, Proceedings of the Association of Asphalt Paving Technologists, p. 391, 1972.
- (6) W. Heukelom, "Observations on the Rheology and Fracture of Bitumens and Asphalt Mixes," Vol. 35, Proceedings of the Association of Asphalt Paving Technologists, p. 358, 1966.
- (7) N. W. McLeod, "A Four-Year Survey of Low Temperature Transverse Pavement Cracking on Three Ontario Test Roads," Vol. 41, Proceedings of the Association of Asphalt Paving Technologists, p. 424, 1972.
- (8) P. S. Kandahl, "Evaluation of Six AC 20 Asphalt Cements by Use of the Indirect Tensile Test," Transportation Research Record, Vol. 712, *Transportation Research Board*, Washington, D.C., p. 1, 1979.
- (9) J. L. Duthie, "Proposed Bitumen Specifications Derived from Fundamental Parameters," Vol. 41, Proceedings of the Association of Asphalt Paving Technologists, p. 71, 1972.
- (10) H. S. Pink et al., "Asphalt Rheology; Experimental Determination of Dynamic Moduli at Low Temperature," Vol. 49, Proceedings of the Association of Asphalt Paving Technologists, p. 64, 1980.
- (11) W. J. Gaw, "The Measurement and Prediction of Asphalt Stiffness at Low and Intermediate Pavement Service Temperatures," Vol. 47, Proceedings of the Association of Asphalt Paving Technologists, p. 457, 1978.
- (12) D. N. Little et al., "Design and Characterization of Paving Mixtures Based on Plasticized Sulfur Binders—Engineering Characterization," Report No. FHWA/RD 85/032, *Federal Highway Administration*, Washington, D.C., July 1984.
- (13) ASTM E813, "J_{ik}, A Measure of Fracture Toughness," Vol. 03.01, 1984.
- (14) "Guide to Modern Methods of Instrumental Analysis," T. H. Gow ed., *John Wiley and Sons, Inc.*, New York, p. 130, 1972.
- (15) D. A. Anderson and E. L. Dukatz, "Fingerprinting Versus Field Performance of Paving Grade Asphalts," Report No. PTI 8319, *Pennsylvania State University Research*, August 1983.
- (16) J. Y. Welborn, E. R. Oglio, and J. A. Zenewitz, "A Study of Viscosity-Graded Asphalt Cements," Vol. 35, Proceedings of the Association of Asphalt Paving Technologists, pp. 19-60, 1966.
- (17) "SAS Users' Guide: Statistics," 1982 ed., *SAS Institute, Inc.*, Cary, N.C.
- (18) C. Daniel and F. S. Wood, "Fitting Equations to Data," 2d ed., *John Wiley and Sons, Inc.*, New York, 1980.
- (19) W. J. Dixon and F. J. Massey, "Introduction to Statistical Analysis," 2d ed., *McGraw Hill Book Company, Inc.*, New York, 1957.

Brian H. Chollar is a research chemist in the Materials Technology and Chemistry Division, Office of Engineering and Highway Operations Research and Development, FHWA. Currently, he is the project manager of FCP Project 3C, "Calcium Magnesium Acetate (CMA) as an Alternate Deicer." He also manages contracts and conducts staff studies in several areas of materials research including delineation, alternative binder materials, chemistry of asphalts, and additives to asphalt. Before joining FHWA in 1974, Dr. Chollar was a research chemist at NCR Corporation involved with synthesis and analysis of organic materials including liquid crystals, organo-metallic compounds, and substituted porphyrins.

John G. Boone is a research chemist in the Materials Technology and Chemistry Division. He has more than 30 years experience in determining the chemical and physical characteristics of organic and inorganic binders and related highway materials. He has been involved in cooperative testing with scientific societies and State highway departments concerning materials and testing procedures for specification requirements. Before joining the Bureau of Public Roads in 1953, Mr. Boone was employed by the National Bureau of Standards, conducting conformance to specification tests on bituminous paving materials used by the District of Columbia government.

Warren E. Cuff, a graduate chemist from Morehouse College, Atlanta, Georgia, worked as a physical scientist aid during the summer of 1984 for the Materials Technology and Chemistry Division. During that summer, Mr. Cuff conducted high-pressure gel permeation chromatography measurements of asphalt solutions and data calculations to obtain the chromatographic properties of asphalt.

Ernest F. Bailey is a research soil scientist in the Materials Technology and Chemistry Division. He participates in staff research programs involving studies of various physical and chemical properties of deicing salts, delineation materials, asphaltic cements, and other binder materials. Mr. Bailey performs various physical, chemical, and mineralogical tests associated with the chemistry of these and other highway materials.



Residual Driving Stresses and Vertically Loaded Piles in Cohesionless Soils

by
Jean-Louis Briaud and Albert F. DiMilio

This article is based on a paper presented at the March 1984 Federally Coordinated Program (FCP) of Highway Research, Development, and Technology conference in McLean, Virginia. Federal Highway Administration (FHWA) pile foundation research is included under FCP Project 5P, "Foundations and Earth Structures." The main focus of the pile foundation research is to develop improved design and predictive techniques for single piles and pile groups. Current research involves laboratory and full-scale field experiments to better define single pile behavior as a function of pile geometry, material type, and soil properties. A simple, reliable method for relating single pile behavior to group behavior also will be developed. A complete understanding of residual driving stresses in piles is necessary to accurately define pile-soil interaction. Current design procedures will be adjusted to incorporate residual driving stresses as warranted by the experimental analysis.

Introduction

During a hammer blow, a pile moves downward, rebounds, and then oscillates around a final position. At its final position, the pile is in equilibrium under a certain point load and a certain friction load, each of which cancels out because the load at the pile head is zero. This process is repeated for each blow. Figure 1 shows the residual load distribution in the pile at final penetration.

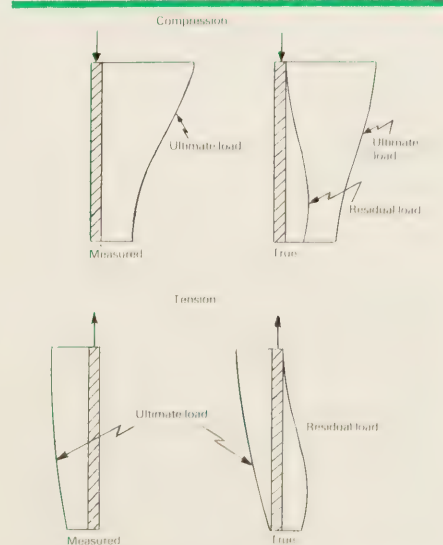


Figure 1. Measured and true load in a driven pile.

During the downward movement of the pile, the pile soil friction acts upward to resist penetration; the point soil resistance also acts upward. During the rebound that follows, the soil under the point pushes the pile back up while the pile decompresses elastically. These two rebound components create enough upward movement to reverse the pile soil friction which now acts downward at least in the upper portion of the pile. Equilibrium is reached when enough of the friction stresses have reversed themselves to keep the bottom of the pile stressed against the soil.

This explains how the unloading characteristics of the point and friction transfer curves (q_w and f_w curves) and the elastic characteristics of the pile govern the residual stresses phenomenon. Also, this phenomenon can be caused by reconsolidation after driving if relative movement between the pile and soil occurs. In sands, for example, a significant residual point load can exist because point capacities are large and because little movement is needed to unload the friction transfer curve; much more movement is needed to unload the point transfer curve.¹

¹J. L. Briaud, L. M. Tucker, R. L. Lytton, and H. M. Coyle, "The Behavior of Piles and Pile Groups in Cohesionless Soils," Report No. FHWA RD 84-007, Federal Highway Administration, Washington, D.C., October 1983. Unpublished report.

Although the existence of residual stresses has been known for a long time, the residual stresses have not been routinely included in pile design. (1, 2)²

Why Are Residual Stresses Important?

In a conventional load test on an instrumented pile, the following testing sequence usually is observed: The pile is instrumented and then driven, the instrumentation is zeroed, and finally, the load test is performed. Zeroing the instrumentation is equivalent to assuming that no stresses exist in the pile after driving. Therefore, in a conventional load test residual stresses are not obtained.

The differences for a compression test and a tension test in load distribution in the pile between the measured loads as described above and the true loads that exist in the pile are shown in figure 1. The interpretation of the results from a conventional compression test lead to a point load that is lower than the true point load and to a friction load that is higher than the true friction load. The interpretation of the results from a conventional tension test, on the other hand, leads to a point load that is larger than the true point load, which is zero, and to a friction load that is smaller than the true friction load. Because the residual stresses are neglected, all the predictive methods based on these conventional load test results are in error. Residual stresses must be considered to develop a valid predictive method.

Residual Stresses Affect Pile Length

In an uninstrumented pile load test, residual stresses cannot be measured. This is not important if the test is performed only to verify the capacity of the design pile. Because the measured top load and top movement are correct, there is no need to know the residual stresses. However,

if the results of the pile load tests are extrapolated to a pile of a different length, the residual stresses must be considered because the stresses affect the load distribution.

For piles in sand, the point capacity becomes more important as the piles decrease in length. Because the point capacity is larger after considering residual stresses, short piles will become shorter. As the piles become longer, the friction becomes more important. Because the friction is smaller after considering residual stresses, long piles will need to be longer to carry the same capacity.

However, a pile rarely is driven through 100 ft (30 m) or more of sand. Commonly, long piles are driven through clay with the tip seated in a sand layer. Measurements on piles in clay indicate that residual point loads in the pile are less than 5 percent of the ultimate pile capacity; in sand, however, they may be more than 20 percent of the ultimate pile capacity. Thus, residual stresses should not significantly affect the current prediction methods for pile capacity in clay. Consequently, a pile driven through clay into sand should carry more load than predicted without considering residual stresses. Considering residual stresses does not reduce the friction in the clay; however, their consideration does increase the point bearing in the sand. In most cases, therefore, the consideration of residual stresses results in shorter pile length.

Residual Stresses From Pile Load Tests

The following methods can be used to measure or estimate residual stresses from pile load test data. Method 1 was found to be the most reliable and Method 4 the least reliable.

Method 1: Read instrumentation before and after driving: The most direct method of measuring residual loads is to calculate them from instrument readings taken before and after driving. While the pile is hanging under its own weight in driving position, zero the instrumentation. After final penetration, read the instrumentation and calculate the residual loads directly.

All other methods consist of zeroing the instrumentation after the pile is driven and of determining the residual load by using a combination of testing sequence and theoretical reasoning.

Method 2: Hunter-Davisson method (1):

This method involves a specific testing sequence during the load test followed by a special reasoning sequence during the data analysis. The testing sequence consists of the following steps:

1. Drive the pile.
2. Zero the instrumentation.
3. Load the pile to failure in compression and read the instrumentation.
4. Unload the pile to zero top load and read the instrumentation.
5. Zero the instrumentation.
6. Load the pile to failure in tension and read the instrumentation.
7. Unload the pile to zero top load and read the instrumentation.

The reasoning and analysis sequence consists of the following steps, which are shown in figure 2:

1. Curve 1 represents the measured ultimate compression load distribution, assuming no stresses in the pile at start of test.
2. Curve 2 represents the measured compression load distribution after complete release of the applied compressive load, assuming no stresses in the pile at start of test.
3. Curve 3 represents the measured ultimate tension load distribution, assuming no stresses in the pile at start of test.
4. Curve 4 represents the measured tension load distribution after complete release of the applied tensile load, assuming no stresses in the pile at start of test.
5. Assuming that no residual stresses exist at the end of the tension test, curve 4 represents the residual compressive loads for the test and, when subtracted from curve 3, gives curve 5, the adjusted tension load distribution.
6. Curve 4 includes the original compressive residual loads in the pile from driving before the compression test and the residual loads induced by the compression test. Subtracting curve 2 from curve 4 gives curve 6, the original compressive residual loads in the pile.

²Italic numbers in parentheses identify references on page 17.

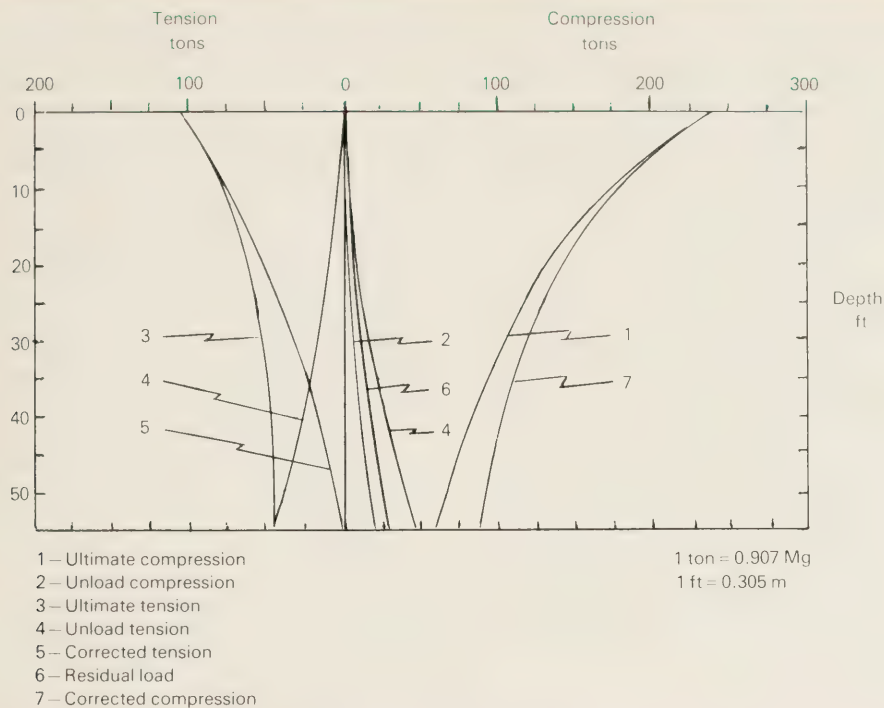


Figure 2.—The Hunter-Davisson method to obtain residual loads.

Table 1.—Comparison of methods of obtaining residual loads from load test data

Site	Pile	Method 1			Method 2			Method 3			Method 4	
		Q_{res}	Q_p	Q_s	Q_{res}	Q_p	Q_s	Q_{res}	Q_p	Q_s	Q_p	Q_s
Arkansas River	1				37	87	85	32	82	90	77	95
	2				45	120	122	62	137	105	127	115
	3				48	163	109	64	179	93	152	120
	7H				25	85	158	25	85	158	175	67
	10				10	83	159				134	108
	16				40	93	82	33	86	89	97	78
Low Sill	2							29	179	241	225	195
	4							37	125	315	215	225
	5							29	54	91	61	84
	6							51	186	244	245	185
Gregersen	A	3.3	6.5	20.5							17	10
	D/A	5.3	12.0	39.0							24	27
	C	1.3	4.5	29.5							18	12
	B/C	5.3	7.0	41.0							25	23
Sellgren	AI	7.0	66.0	11.5								
	AII	13.0	33.5	109.0								
Lock and Dam 26	3IP-III5H				24.5							
Ogeechee River	H-15										248	173

1 ton = 0.907 Mg

7. Adding curve 6 to curve 1 gives curve 7, the adjusted compression load distribution.

This method assumes that the tension test induces no residual loads. However, this assumption is incorrect; the error is zero at the top and bottom of the pile and peaks toward the middle of the pile where the residual tension load can be 25

percent of the ultimate tension load.³ Although this method accurately predicts residual point load, it gives erroneous residual friction stresses distribution.

³J. L. Briaud, L. M. Tucker, R. L. Lytton, and H. M. Coyle, "The Behavior of Piles and Pile Groups in Cohesionless Soils," Report No. FHWA RD 84-007, Federal Highway Administration, Washington, D.C., October 1983. Unpublished report.

Method 3: No unloading reading method: The testing sequence used for a load test often is not as rigorous as the testing sequence required in the Hunter-Davisson method. Method 3 is used when the instrumentation was not read after unloading the pile; that is, when steps 4 and 6 of the Hunter-Davisson method were not performed. Consequently, curves 2 and 4 in figure 2 are not available for analysis. In this method the tension load at the point is assumed to be the residual compressive load at the point after driving. This assumes that the change in residual loads created by the compression test is negligible. For this method, curve 4 is a line joining the point load of curve 3 and zero load at the top.

Method 4: No instrumentation method: When only the load and movement of a pile are measured at the top, the load distribution in the pile cannot be obtained. In Method 4 the ultimate tension load is assumed to be the ultimate friction load in compression. This friction load is subtracted from the ultimate compression load to give the ultimate point load, which includes but does not equal the residual load in the pile.⁴ Because this method does not adequately estimate the true residual load, Method 4 was not used in further analysis in this study.

Table 1, which is based on the one-tenth of the pile diameter (0.1D) failure criterion, summarizes the results of the four methods for a series of load tests.⁵ In a comparison of Methods 2 and 3 for five piles at the Arkansas River site, the residual load given by Method 3 averaged 13 percent higher than that given by Method 2. This discrepancy is because Method 3 assumes no additional residual loads were induced in the piles during the compression test. This assumption, however, is false. Methods 1, 2, and 3 yield a compressive side friction load, whereas Method 4 gives the tensile friction load. A comparison of results from

⁴Ibid.

⁵Ibid.

Method 4 with the results from Methods 1, 2, and 3 shows that on the average of 14 pile load tests the friction in tension is only 70 percent of the friction in compression. This percentage varies from 40 percent to 110 percent and is lowest for short piles, H piles, and tapered piles.⁶

To identify the important parameters affecting pile behavior under load and formulate a pile design method that incorporates residual stresses, various correlations were performed using the pile and soil data from documented load tests on instrumented piles that were hammer driven and load tested vertically. The resulting data base was analyzed to determine the load transfer characteristics of the soil, including the effects of residual driving stresses where the data were available. The literature review identified ten sites with a total of 35 instrumented piles.⁷ (3)

Because of a lack of other soil data at the sites, only the standard penetration test (SPT) N values (blow counts) were used in the correlations. Uncorrected N values were used because correction methods are not universally accepted. The correlations were performed in three main categories: Residual driving stresses, point pressure-point movement characteristics, and side friction-pile movement characteristics. The majority of the load tests did not measure residual stresses in the pile. When measurement data were not available, the residual stresses were determined from the correlation described above.

A Look at the Future

The pile design method discussed above is a step forward, but further research is needed in this area. The first important step is to measure residual stresses as often as possible when a pile is load tested. This measuring should occur even on routine load tests, provided a simple measurement method can be developed, and should be a contract specification for major jobs so a data base can be collected from which an improved design method can be developed.

The testing method for measuring residual stresses and the design method to include residual stresses in pile length calculations should be developed from carefully controlled research experiments. The design method then could be adjusted or verified on actual jobs with the testing method.

The second important step is to ensure that any drivability study with the wave equation program simulates at least five consecutive blows of the hammer as opposed to a single blow (fig. 3). (4) Common practice is to simulate a single blow of the hammer on the pile, which does not properly consider residual stresses that are induced by the first blow and seem to stabilize after three blows.⁸ A pile free of residual stresses will drive harder than a pile affected by the residual stress distribution.

Other aspects to be researched are the evolution of residual stresses with time, the change in residual stresses

caused by the driving of additional piles in a group, and the distribution of residual stresses in very long piles.

Current FHWA research on residual driving stresses in piles in sands involves carefully controlled field experiments to determine the effect of pile type (taper, material, and stiffness) on the development of residual stresses. Correlations will be developed between settlement, load transfer behavior, relative stiffness, length to diameter ratios, soil properties, and other geometric and materials factors. The relative development of residual stresses in low and high displacement piles will be assessed and the influence on pile design methods evaluated. Currently used methods for predicting the behavior of single piles will be applied to the design of test piles and a comparison made between the predicted and measured behavior. Each test pile will be instrumented and dynamic measurements will be made during driving.

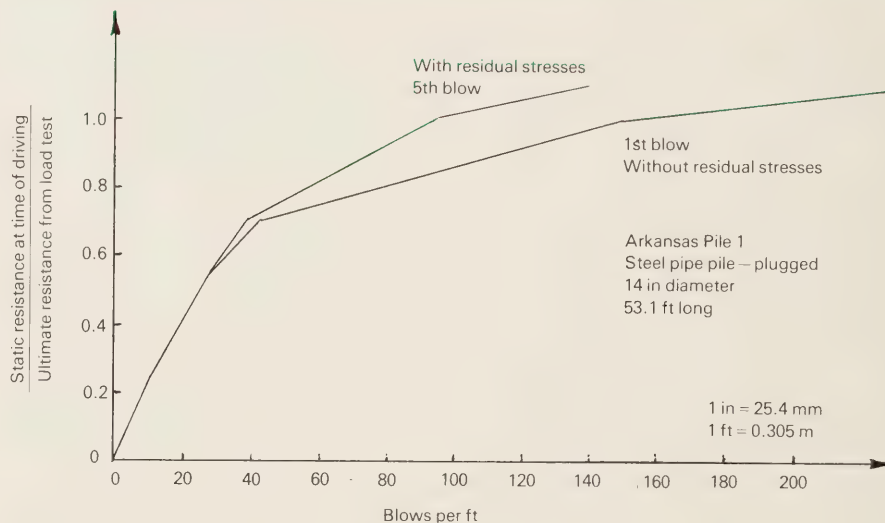


Figure 3. — Influence of residual stresses on drivability analysis with the wave equation.

⁶Ibid.
⁷Ibid.

⁸Ibid.

Driving resistance records and ground response will be measured. Tension (uplift) tests will be performed after each compression test. The correlations developed from the measured and computed results will be used to refine and/or modify current predictive techniques.

Summary

Significant residual point loads can exist in piles driven in sands. The stresses caused by the residual loads are routinely neglected in current pile design methods. Consideration of residual stresses can result in significant cost savings when pile lengths are reduced. Little or no effect is involved in pile design for clay soils.

A method to incorporate residual stresses in pile design for sands was developed from correlations with SPT N values. These correlations were used to predict the entire load settlement curve for a pile with the new residual stress method.

The phenomenon of residual stresses in a pile takes place upon unloading of that pile after either a hammer blow, a compression test, or a tension test. A theoretical formulation of this unloading process, based on the fundamental differential equation, indicates the following influences of various factors:

- The longer the pile, the larger the residual point load.
- The more compressible the pile, the larger the residual point load.
- The steeper the unloading slope of the friction transfer curve, the larger the residual point load.
- The softer the unloading slope of the point transfer curve, the larger the residual point load.

The distribution of residual loads and residual stresses in a pile is directly related to distribution of ultimate loads and ultimate stresses in that pile, and residual loads after a tension test are not zero but are much smaller than those after a compression test.

REFERENCES

- (1) A. H. Hunter and M. T. Davisson, "Measurement of Pile Load Transfer, Performance of Deep Foundations," ASTM STP 444, 1969.
- (2) D. M. Halloway, G. W. Clough, and A. S. Vesic, "The Mechanics of Pile-Soil Interaction in Cohesionless Soils," *Corps of Engineers*, Vicksburg, Miss., 1975.
- (3) J. L. Briaud and L. M. Tucker, "Piles in Sand: A Method Including Residual Stresses," *ASCE Journal of Geotechnical Engineers*, Vol. 110, No. 11, November 1984.
- (4) J. L. Briaud and L. M. Tucker, "Residual Stresses in Piles and the Wave Equation," *Proceedings of the ASCE Symposium on Analysis and Design of Pile Foundations*, San Francisco, Calif., October 1984.

Jean-Louis Briaud is an associate professor of civil engineering at Texas A&M University in College Station, Texas. Dr. Briaud also is president of Briaud Engineers and does consulting work both in Canada and the United States on various topics including slope stability, highway embankments, oil tank foundations, deep foundations, and onshore and offshore pressuremeter testing.

Albert F. DiMillio is a geotechnical research engineer in the Construction, Maintenance, and Environmental Design Division, Office of Engineering and Highway Operations Research and Development, FHWA. Mr. DiMillio is project manager for FCP Project 5P, "Foundations and Earth Structures." Prior to his present position, he served as an area engineer in FHWA's Indiana Division Office and as the Regional Geotechnical Specialist in Region 5, Homewood, Illinois.



Long Term Monitoring of Pile Foundations

by
Carl D. Ealy and Albert F. DiMillio

Introduction

The Federal Highway Administration (FHWA) is conducting a comprehensive research program to develop improved design procedures for bridge foundations. Improving the design of pile foundations is a major focus of this research. Several studies have been completed that have resulted in new design methods, which for the most part have been validated based on published data or on a few carefully conducted field tests. However, to determine the application limits or to refine or modify these new methods, the methods must be applied to independent data sets covering as wide a range of conditions as possible. The effect of construction on applying analytical methods to the design of service foundations must be considered. Very little high quality data are available in the literature on the effects that construction activities, such as driving adjacent piles, inadvertent batters, deformed piles, and changes in soil properties because of pile installation, have on predictive methods.

It is equally important that data be obtained on the long term behavior of piles and pile groups, especially for piles subjected to downdrag loads or other unusual loading conditions. Knowledge of inservice behavior also may lead to substantial savings on projects with similar soil and site conditions.

This article presents the results of load tests and a long term monitoring program on a bridge along the Natchez Trace Parkway and the Douge Creek Bridge in Fort Belvoir, Virginia. Also presented are preliminary results from the West Seattle Bridge to obtain information on the short and long term load settlement and load transfer behavior of inservice piles.

FHWA monitored the Natchez Trace Parkway and Douge Creek bridges in cooperation with the Eastern District Federal Division and monitored the West Seattle Bridge in cooperation with the City of Seattle.

Natchez Trace Parkway

Site description

The test site, located at Big Brown Creek near Tupelo, Mississippi, along the Natchez Trace Parkway, is underlain by 25 to 30 ft (7.6 to 9.1 m) of loose to medium silts and fine sands, which overlie a dense sand layer of undetermined thickness (fig. 1). Dutch Cone soundings and Standard Penetration Test (SPT) data indicate low shear resistance within the upper 30 ft (9.1 m) (fig. 2). Consolidation of the 10 ft (3.0 m) high approach fills was estimated to take 381 days for 95 percent consolidation. As a result of consolidation, the abutment piles were subjected to an estimated 25 tons (22.8 Mg) of downdrag load. The test pile is one of six H piles (12HP53) supporting the west abutment of the bridge.

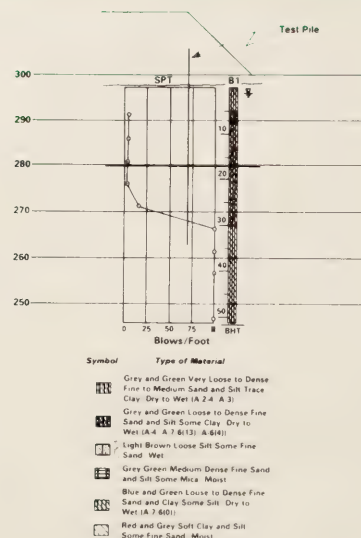


Figure 1. — Location of test pile and soil profile (Natchez Trace Parkway).

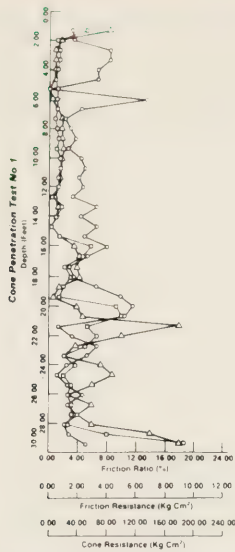


Figure 2.—Dutch Cone soundings (Natchez Trace Parkway).

Instrumentation

Pile instrumentation consisted of 10 levels of strain gages evenly spaced along 47 ft (14.3 m) of the test pile to measure load transfer (fig. 3). A wire extensometer measured tip movement during static load testing. Bondable resistance strain gages were placed in a half-bridge configuration at each gage level. Two active gages were located diametrically opposite each other on the center of either side of the pile web. Two dummy gages for temperature compensation were placed on tabs welded to the web and placed in adjacent arms of the bridge. The two half-bridges were joined at the terminal strip to form a full bridge. Several layers of protective coating covered each gage installation, and two steel channels, one welded on each side of the web, protected the gages from damage during driving. The space between the channel sections and web was filled with epoxy. The readout system consisted of a strain indicator and switch and balance box. Before being delivered to the field, the instrumented pile was calibrated in the laboratory to obtain a direct relationship between applied load and gage response.

Installation and load test results

The test pile was installed on October 21, 1980, with a diesel hammer having a rated maximum energy of 25,000 ft-lb (33.9 MJ). Before it was static load tested, the test pile was driven another 1 ft (0.305 m) to its final elevation to evaluate soil setup. The retap of the pile indicated that soil setup or freeze developed approximately 35 tons (31.7 Mg) of additional pile capacity. The pile penetrated the first 10 ft (3.0 m) under the weight of the hammer. From 10 to 29 ft (3.0 to 8.8 m) blow counts were approximately 3 to 6 blows/ft (0.9 to 1.8 blows/m). To this depth, the pile hammer performed erratically because of the low soil resistance. From 29 to 34 ft (8.8 to 10.4 m) of pile penetration, resistance increased significantly.

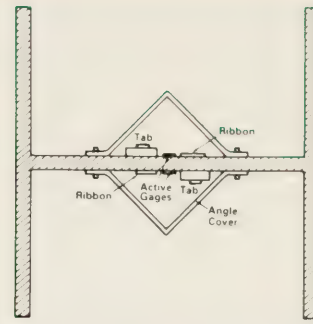


Figure 3.—Cross section through H pile showing typical strain gage installation (Natchez Trace Parkway).

Design criteria called for penetration to 47 ft (14.3 m) or 40 blows/ft (12 blows/m). The blow count criterion was reached at 34 ft (10.4 m) of penetration. Because the strain gages were placed in accordance with an assumed penetration of 47 ft (14.3 m), two levels of gages were above ground and in the plane of the abutment as a result of the short penetration. Rather than drive the pile another 10 ft (3.0 m), which would have required a bigger hammer and negated any need for a load test, driving was continued for an additional 4 ft (1.2 m) of penetration at which point refusal was reached at a blow count of 123 blows/ft (37 blows/m). This allowed one of the two exposed strain gage stations to be salvaged.

Dynamic measurements were taken with a pile driving analyzer during the last 15 ft (4.6 m) of pile driving. The excess piling was cut off and the terminal strip and gage connections carefully reassembled. Of the 10 levels of gages, one level was lost because of the short penetration, and another was lost because water penetrated the protective coating.

Static load testing was conducted on October 28, 1980. Figures 4–6 show load test results and a comparison between computed and measured behavior. The field data were used to evaluate the PILGP1 pile group analysis program developed for FHWA under previous research. (1)¹ Basically, the model will output distribution of loads to heads of piles because of loads applied at the center of the pile cap, individual pile reactions, load distribution along a pile, and load settlement values. The user must input F-Z data, which describe the relationship between skin friction and relative pile movement, Q-Z data, which describe the relationship between the load at the tip of a pile and movement of the pile tip, and pile and soil properties.

Table 1 presents the test pile analysis using F-Z and Q-Z curves determined from criteria suggested in reference 2. F-Z curves were input for three depths—0, 28 ft (8.5 m), and 38 ft (11.6 m)—along the length of the pile. After the load test, the pile was reanalyzed using F-Z and Q-Z curves derived from the measured load distribution data.

¹ Italic numbers in parentheses identify references on page 29.

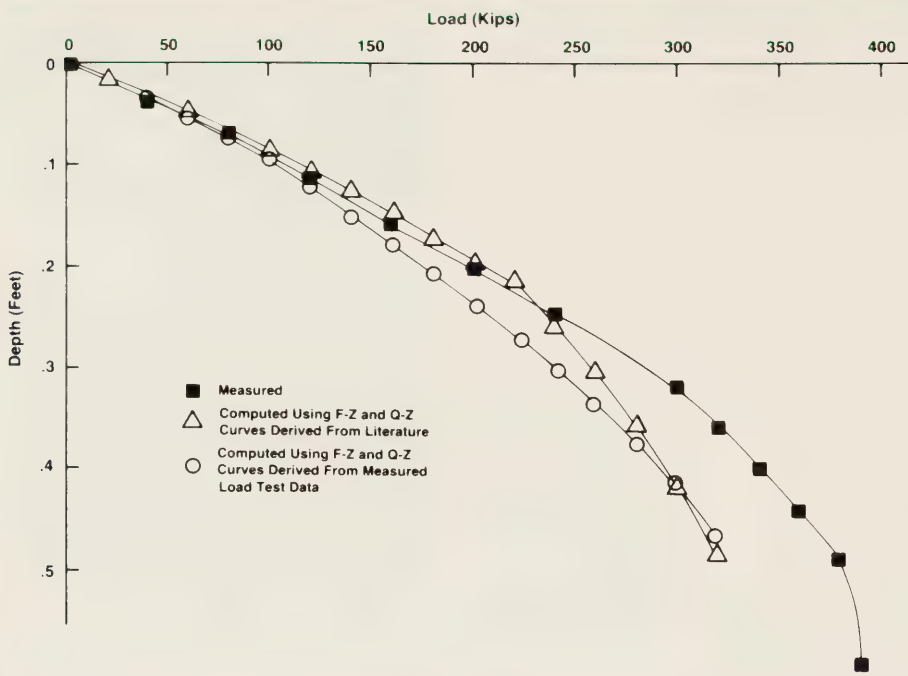


Figure 4.—Comparison between measured and computed load settlement (Natchez Trace Parkway).

Table 1.—F-Z and Q-Z data used in PILGP1 analysis¹ (Natchez Trace Parkway)

Z (in)	0 depth F (psi)	28 ft depth F (psi)	38 ft depth F (psi)	Z (in)	Q (lb)
0.0	0.0	0.0	0.0	0.0	0.0
0.025	0.0	5.177	7.39	0.0375	99,973
0.05	0.0	6.786	9.638	0.124	146,766
0.075	0.0	7.733	11.041	0.188	168,336
0.10	0.0	8.409	12.005	0.251	185,405
0.15	0.0	9.228	13.175	0.311	199,980
0.20	0.0	9.614	13.725	0.375	211,600
0.225	0.0	9.696	13.843	10.0	211,601
0.25	0.0	9.722	13.88		
0.10	0.0	9.722	13.88		

¹ F-max and Q-max determined from reference 2.

1 ft = 0.305 m

1 in = 25.4 mm

1 psi = 6.89 kPa

1 lb = 0.454 kg

For this analysis, F-Z curves were input for depths of 0, 14.5 ft (4.4 m), 29.5 ft (9.0 m), 34.5 ft (10.5 m), and 38 ft (11.6 m). Q-Z values were derived by extrapolating the failure load distribution curve for the last two strain gage stations to the pile tip to determine Q-max and applying the formulas suggested in reference 2.

Table 2 shows the F-Z and Q-Z data used for the reanalyzed solution. The F-Z and Q-Z curves described above do not reflect residual driving stresses in the piles; that is, the analyses using these curves assume no loads in the pile after driving and before the application of incremental test loads. Theoretically, the top of the pile load settlement data should not be affected; however, the measured load transfer data would be in error by an amount corresponding to the magnitude and distribution of the residual shaft and point loads. Therefore, the following results compare the "apparent" load transfer behavior.

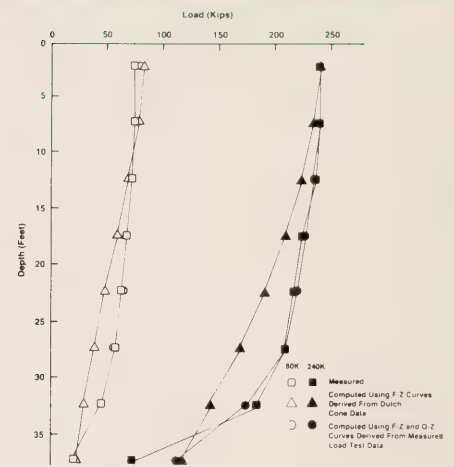


Figure 5.—Comparison between measured and computed load distribution (Natchez Trace Parkway).

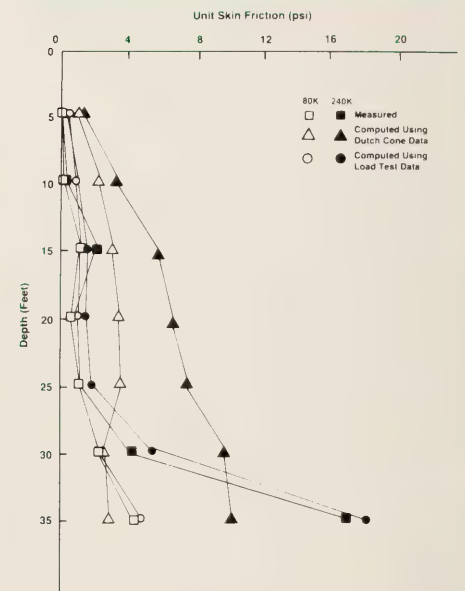


Figure 6.—Comparison between measured and computed unit skin friction (Natchez Trace Parkway).

Figure 4 compares the measured and computed load settlement. Measured failure load was taken as 197 tons (179 Mg) and the corresponding total settlement was taken as 0.45 in (11.4 mm). The criterion curve correlates well with the measured curve with approximately a 5 percent difference between the computed and measured curve for loads up to and slightly beyond the working load range (98 tons [89 Mg]). The reanalyzed curve coincides with the measured curve for loads up to half the working load then deviates to an overprediction of settlement of approximately 3 percent at the working load level after which the difference between the reanalyzed and measured curve increases rapidly.

**Table 2.—F-Z and Q-Z data used in PHLGPI analysis¹
(Natchez Trace Parkway)**

Z (in)	0 depth F (psi)	24.5 ft depth F (psi)	29.5 ft depth F (psi)	34.5 ft depth F (psi)	38 ft depth F (psi)	Q (lb)	Z (in)
0.0	0.0	0.0	0.0	0.0	0.0	20,104	0.00
0.02	0.0	0.40	2.5	8.7	8.7	51,377	
0.04	0.0	1.25	3.5	13.2	13.2	105,000	0.08
0.06	0.0	1.42	4.3	16.0	16.0	142,246	0.10
0.08	0.0	1.46	4.85	17.48	17.48	189,871	0.17
0.10	0.0	1.48	5.2	18.10	18.10	191,106	0.20
0.12	0.0	1.49	5.5	18.50	18.50	191,100	1.00
0.14	0.0	1.50	5.21	18.70	18.70		
0.20	0.0	1.50	5.52	19.20	19.20		
1.0	0.0	1.50	5.52	19.20	19.20		

¹From measured load transfer data.

1 ft = 0.305 m

1 in = 25.4 mm

1 psi = 6.89 kPa

1 lb = 0.454 kg

Figures 5 and 6 compare the computed load distribution and unit skin friction to the measured values for loads of 80 and 240 kips (36.3 and 108.9 Mg). The curves clearly show that the upper 25 ft (7.6 m) of soil provides little frictional support and the upper 12 ft (3.7 m) provides essentially zero support. This was expected because of the low frictional resistance in the upper silt and clay layers. Significant load transfer did not occur until a depth of 25 ft (7.6 m), which corresponds approximately with the top of the dense sand layer. Basically, the data indicate that the tip of the pile carries 45 percent of the applied load, the lower quarter of the pile carries 86 percent, and the lower 10 to 15 ft (3.0 to 4.6 m) of soil carries 20 percent. Under the proposed working load of 98 tons (89 Mg), the relative distribution between tip and side resistance is essentially the same with slightly less load reaching the tip.

In contrast to the load settlement curves, the reanalyzed load distribution curves nearly coincide with the measured load distribution and unit skin friction curves while the criterion curves show only fair to poor agreement.

Long term monitoring

Figure 7 summarizes the load changes measured in the service pile and the major construction events. A number of apparently anomalous load readings taken throughout the construction period probably reflect reading errors rather than actual load changes in the pile. A rainstorm soaked the terminal strip and readout equipment 95 days after the load test. For several weeks thereafter, gage readings did not appear to reflect real load changes in the pile. Generally, however, the curves correspond qualitatively with the major construction events. Initial readings were taken immediately after the load test on October 28, 1980, and subsequent readings were taken on a weekly basis for 700 days.

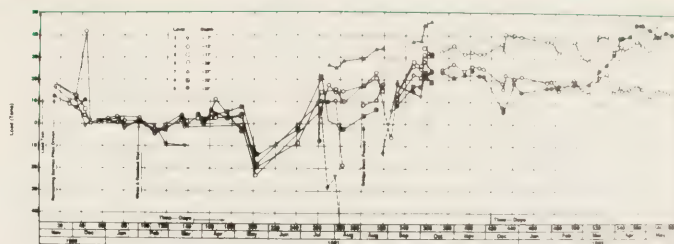


Figure 7.—Load change with time (Natchez Trace Parkway).

After the load test, all gage levels, except the last gage (located 1 ft [0.305 m] above the pile tip), indicated tension loads of approximately 9 tons (8 Mg). The last gage level indicated that approximately 9 tons (8 Mg) of compressive load remained in the piles near the tip. Between the end of the load test and before driving the remaining service piles, the load increased to 16 to 20 tons (14.5 to 18.1 Mg) at levels 2 through 8. The load at level 9 increased to 12 tons (10.9 Mg). During this period, the only construction activity near the abutment was the hauling and compacting of the approach fill. However, this activity was several hundred feet from the abutment site and theoretically should have the opposite effect, if any, on the load distribution.

The abutment was poured on December 12, 1980. During this period, the loads generally decreased at each level to between 5 and 10 tons (4.5 to 9.1 Mg). Loads continued to decrease to 0 to 5 tons (0 to 4.5 Mg) and remained at this level for the next 85 days. Embankment construction began in August 1980 and was approximately 95 percent complete at the time of the load test. Assuming that the rate of consolidation predictions presented earlier are correct, excess pore pressure levels would still be high at this time. The decreased and sustained low loads carried by the pile beginning shortly after the abutment was poured may have resulted from the additional fill construction near the abutment.

Low load levels, recorded for the next 55 days, gradually increased to between 5 and 10 tons (4.5 and 9.1 Mg) for the next 50 days. During this time, the approach fill was completed. The consolidation and negative skin friction may have contributed to the observed load increases.

As discussed previously, negative readings were recorded for all gage levels between day 200 and 240. A review of the construction logs did not indicate unusual construction activity, severe weather changes, or other physical conditions that might account for the abrupt changes in load distributions. Therefore, the recorded loads are assumed to reflect reading error rather than physical changes in the pile load distribution.

The placing of concrete girders between spans 1 and 2 began July 6 (day 245), which corresponded with a dramatic increase in load at all levels. A dramatic increase occurred again when the bridge deck was poured August 28, 1982 (day 300), also the beginning of very erratic load distribution with depth readings as shown in figure 7.

For clarity, figure 7 only shows gage levels 4, 6, and 9 from day 391 to 591. These levels are located at -12, -22, and -37 ft (-3.7, -6.7, and -11.2 m) respectively. Located in the soil strata with relatively low shear strength, the first two levels theoretically should indicate low load transfer to the soil. The gage level 9 is located 1 ft (0.305 m) above the tip about 7 or 8 ft (2.1 or 2.4 m) into the higher shear strength material. From day 329 through 591, the load at level 4 generally increased slowly from approximately 25 to 35 tons (22.7 to 31.6 Mg) although considerable fluctuation existed. Also, in level 6 the load fluctuates from 20 to 25 tons (18.1 to 22.7 Mg) from day 328 to 591. In contrast, the loads at level 9 remained from 20 to 25 tons (18.1 to 22.7 Mg) with some fluctuation; from day 521 to 560 the loads increased to approximately 45 tons (40.8 Mg) then leveled to about 40 tons (36.3 Mg). Only minor construction activity occurred during this period and is not thought to have contributed to the load changes.

Figure 8 shows the load distributions with depth corresponding to the major construction activities. As discussed previously, the accuracy of a number of the gage readings is uncertain. In addition, the lack of pore pressure and corresponding settlement data on the soil underlying the fill preclude quantitative correlations between the construction activity and the change in load distribution. However, the load distribution change with depth and with construction events corresponds with expected behavior—little load transfer in the upper 25 ft (7.6 m), with most of the load transferred to the pile tip.

Gage readings continued for 729 days after load testing. Beginning with day 600, however, the data indicated large negative loads at all levels. These anomalous readings again were attributed to non-pile soil-related factors such as temperature changes, gage creep, and unknown residual stress effects.

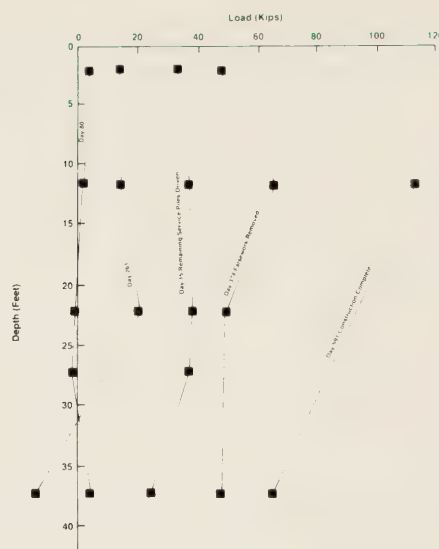


Figure 8. — Load distribution change with time (Natchez Trace Parkway).

Douge Creek Bridge, Fort Belvoir, Virginia

Site description

The bridge site lies in the Atlantic coastal plain geologic province, which is underlain by gravels, sand, silt, and clay soils developed from alluvial deposits. Boring logs indicate the subsurface profile consists of 30 ft (9.1 m) of soft to stiff blue clay, underlain by loose sand for an undetermined depth. Dutch Cone soundings are summarized in figure 9. Service piles at pier No. 1, where the test pile is located, are fluted monotubes 68 ft (20.7 m) embedded length with the bottom 33 ft (10.1 m) having a 0.25 in./ft taper. The abutment piles are 12HP53 H piles. Design loads for the pier piles and the abutment piles are 89 tons (80.7 Mg) and 66 tons (59.9 Mg) respectively.

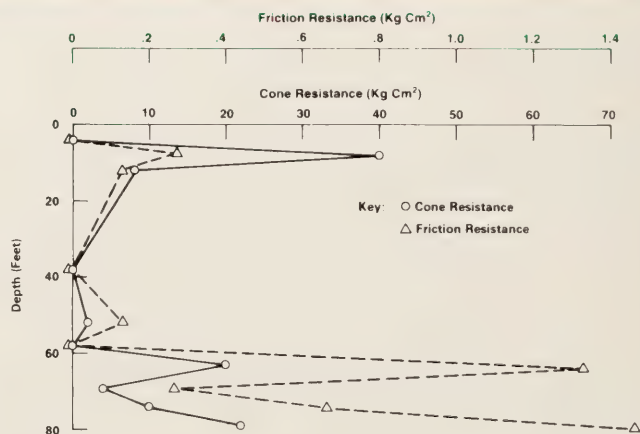


Figure 9. — Dutch Cone soundings (Douge Creek Bridge).

Instrumentation

Figure 10 shows the pile instrumentation. Eight levels of strain gages were installed on a central pipe and then lowered into the monotube after the pile was driven. Most of the gages were located in the lower two-thirds of the pile where most of the load transfer was expected to occur. The instrumentation pipe consisted of an inner and outer steel tube with the gages mounted on the outside of the inner tube.

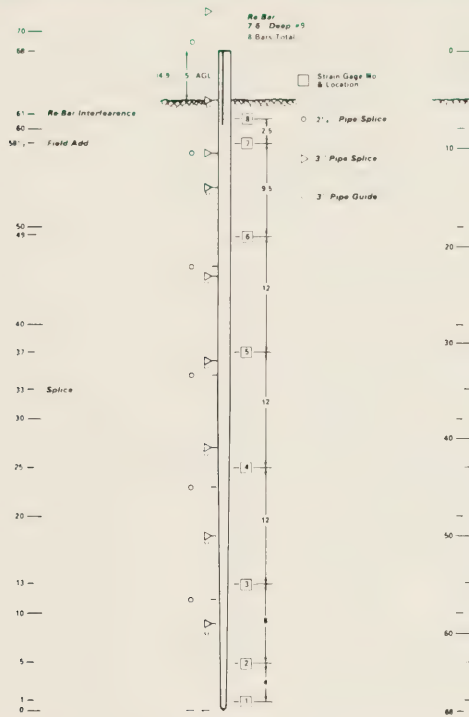


Figure 10. — Pile instrumentation (Dodge Creek Bridge).

Two half-bridges were located at each level (180° apart) and wired to complete a full bridge at the readout box. After the pile was driven, the 3 in (76.2 mm) diameter outer tube and the 2 1/4 in (57.2 mm) instrumented inner tube were assembled in 9 ft (2.7 m) sections and lowered into the center of the monotube. The annular space between the inner and outer tube was filled with a high-strength epoxy. The monotube then was filled with concrete in the space between the 3 in (76.2 mm) diameter tube and the monotube.

Installation and load test results

The test pile, driven on August 26, 1981, with a single acting diesel hammer having a maximum rated energy of 45,000 ft-lb (61.1 MJ), was load tested on September 22, 1981.

The required embedded length for the monotube was reached before the required blow count, the opposite of what occurred at the Natchez Trace Parkway site. Driving was halted for a few moments then resumed. For the next 1 ft (0.305 m) of penetration, blow counts were approximately 10 blows higher than in the previous 1 ft (0.305 m) of penetration. As driving continued, the blow

counts again dropped off. It was decided to drive piles to required lengths regardless of blow count. The low blow counts appear to be caused by reduction in effective stress caused by excess pore pressure, which dissipated rapidly. Figures 11-13 summarize the results of the load test and compare computed and measured behavior.

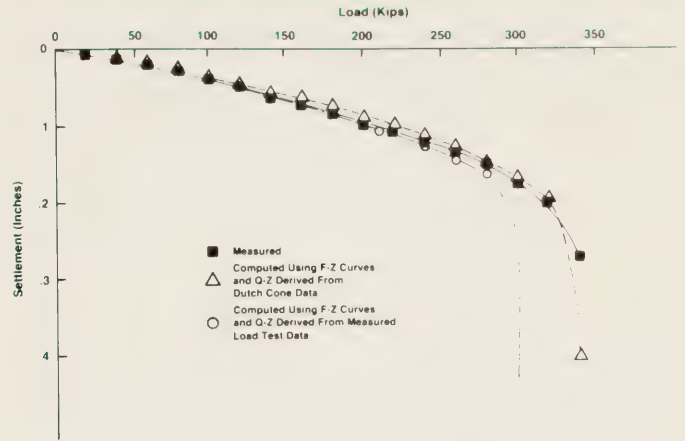


Figure 11. — Comparison between measured and computed load settlement for test pile (Dodge Creek Bridge).

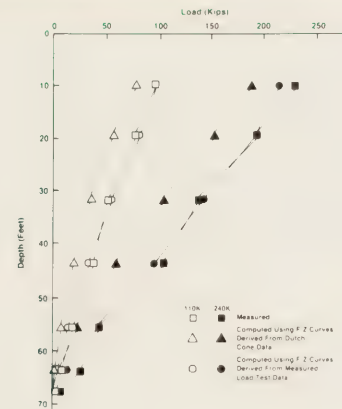


Figure 12. — Comparison between measured and computed load distribution for test pile (Dodge Creek Bridge).

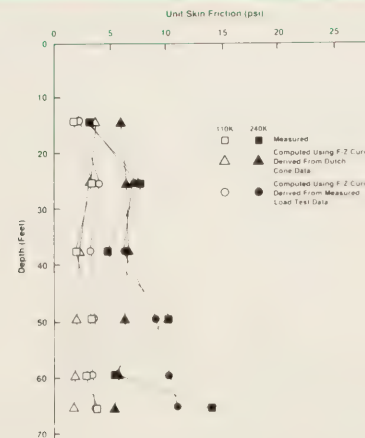


Figure 13. — Comparison between measured and computed unit skin friction (Dodge Creek Bridge).

The load settlement, load distribution, and unit skin friction were computed using the PILGP1 computer model. The pile first was analyzed using input F-Z values based on F values determined from Dutch Cone soundings, with Z_c (the relative displacement at which maximum shear stress [F_{max}] is mobilized) assumed to be 0.25 in (6.4 mm). Two curves, one at the surface and the other at the pile tip, were input. No Q-Z values were input because the pile was designed as a pure friction pile. Table 3 shows the F-Z data used in this analysis.

**Table 3.—F-Z data used in PILGP1 analysis¹
(Dodge Creek Bridge)**

Z (in)	0 depth F (psi)	68 ft depth F (psi)
0.00	0.0	0.0
0.025	3.19	8.52
0.050	4.17	11.11
0.075	4.77	12.73
0.100	5.19	13.84
0.150	5.70	15.19
0.200	5.93	15.82
0.225	6.00	15.96
0.250	6.00	16.00
10.0	6.00	16.00

¹ F-max determined from Dutch Cone data.

1 ft = 0.305 m
1 in = 25.4 mm
1 psi = 6.89 kPa

The pile was reanalyzed after the load test using the measured load transfer data to obtain input F-Z values. Curves were input at the surface and at depths of 14 ft (4.3 m), 25 ft (7.6 m), 37 ft (11.3 m), 49 ft (14.9 m), and 68 ft (20.7 m). Table 4 shows F-Z data used in the reanalysis. Again, the results compare only apparent load transfer behavior because residual load transfer data were not obtained.

Figure 11 compares the measured and computed load settlement relationships. The measured failure load was 166 tons (150.6 Mg), and the corresponding settlement was 0.325 in (8.26 mm). Within the working load range, the Dutch Cone curve underpredicts the settlement slightly but closely agrees with the measured curve well beyond the working load range. The reanalyzed curve

nearly coincides with the measured curve under working loads but begins to deviate sharply from the measured curve beyond this point.

Figures 12 and 13 compare the computed and measured load distribution and unit skin friction curves for applied loads of 55 and 120 tons (49.9 and 108.9 Mg). The measured curve indicates that a nearly linear relationship exists between the load in the pile with depth for the first 35 ft (10.7 m), which marks the end of the straight portion of the pile. The slope then increases sharply with depth. The reanalyzed curve nearly coincides with the measured curve. The curve derived from Dutch Cone data roughly parallels the measured curve but at a 25-percent less load for corresponding levels except for the lower three levels where the curves converge. Figure 13 shows similar correlations for the unit skin friction curves, which indicates that the tapered portion of the pile is more efficient in transferring load to the surrounding soil.

Long term monitoring

Figure 14 summarizes the load changes in the pile from the end of load testing to 2 months after completion of the bridge. All of the gages appeared to function satisfactorily through the first 60 days. Then the test pile was vandalized resulting in the loss of stability in one gage and questionable behavior of another. Of the eight levels of gages, five are thought to have functioned properly throughout the entire monitoring period and to have provided reliable data.

Initial readings were taken immediately after the load test on September 22, 1981 (day 0), followed by weekly readings during construction, and quarterly readings thereafter. The upper three gage levels indicated residual load levels of 10 to 20 tons (9.1 to 18.1 Mg) remaining after the load test. These loads did not change significantly until the west abutment piles (40 ft [12.2 m] from the test pile) were driven on day 12. Readings were taken 2 days before when the east abutment piles (located across the creek 100 ft [30.5 m] from the test pile) were driven. No change in loads was observed during the driving of these piles. During and after the last two west abutment piles

**Table 4.—Data used in PILGP1 analysis¹
(Dodge Creek Bridge)**

Z (in)	0 depth F (psi)	F	14.25 ft depth Z (in)	25 ft depth F (in)	37 ft depth F (in)	Z (in)	68 ft depth F (psi)
0.0	0.0	0.0	0.0	0.0	0.0	0.0	0.0
0.005	0.0	0.6	0.015	3.6	3.6	0.020	10.4
0.015	0.0	1.4	0.030	5.2	5.2	0.030	12.2
0.025	0.0	2.0	0.040	6.1	6.1	0.040	15.40
0.035	0.0	2.35	0.06	7.5	7.5	0.060	17.5
0.045	0.0	2.6	0.075	8.2	8.2	0.070	18.40
0.055	0.0	2.8	0.080	8.4	8.4	0.080	14.0
0.065	0.0	3.10	0.085	8.51	8.51	0.085	19.20
0.075	0.0	3.11	0.090	8.51	8.51	0.090	19.30
1.000	0.0	3.11	1.0	8.51	8.51	1.0	19.30

¹ From measured load transfer data.

1 ft = 0.305 m
1 in = 25.4 mm
1 psi = 6.89 kPa

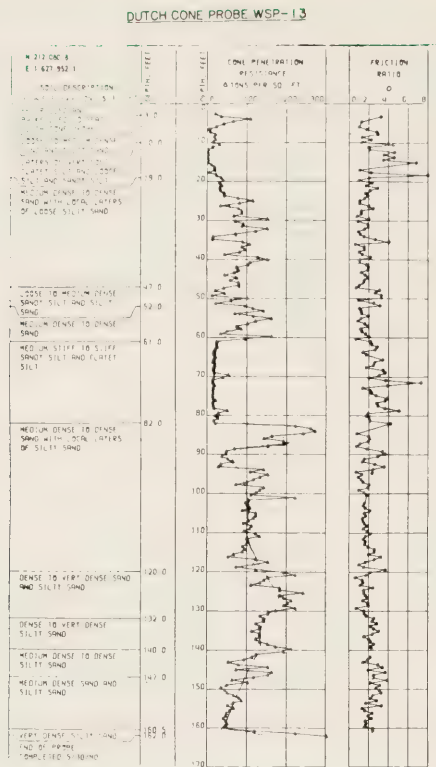


Figure 16. — Dutch Cone soundings (West Seattle Bridge).

with vibrating wire strain gages and telltales at five locations along the length of the pile for load transfer analysis. The load test pile was driven on February 26, 1980, with a diesel hammer having a minimum rated energy of 39,600 ft-lb (53.7 MJ) and a maximum of 94,050 ft-lb (127.5 MJ). Figures 17-19 show the results of the load test and compare computed and measured behavior.

The test pile initially was analyzed using PILGP1 with F-Z and Q-Z input data derived from F-max and Q-max values obtained from the Dutch Cone soundings. It was then reanalyzed using measured load transfer data to derive F-Z and Q-Z input data. Tables 5 and 6 show the number of curves and input values used for each method.

Figure 17 shows the results obtained for the load settlement relationships. The reanalyzed curve correlates well with the measured curve although it slightly underpredicts the settlement. The Dutch Cone curve correlates poorly because of uncertainties in deriving F-max and Q-max values.

Figures 18 and 19 compare the measured and computed load distribution and unit skin friction for applied loads of 200 and 400 tons (181 and 363 Mg) respectively. A fair to good correlation exists between both the Dutch Cone and reanalyzed curve with the measured curves.

Table 5.—F-Z and Q-Z data used in PILGP1 analysis¹ (West Seattle Bridge)

Z	0 depth F (psi)	Z	30 ft depth F (psi)	60 ft depth F (psi)	100 ft depth F (psi)	Q (lb)	Z (in)
0.0	0.0	0.0	0.0	0.0	0.0	0.0	0.0
0.010	0.0	0.050	1.20	3.20	2.60	66,840	0.03
0.030	0.0	0.100	2.20	4.70	4.00	84,255	0.06
0.040	0.0	0.150	3.40	6.00	4.80	99,850	0.10
0.072	0.0	0.200	4.20	7.40	5.60	114,320	0.15
0.095	0.0	0.250	5.0	8.60	6.40	125,795	0.20
0.125	0.0	0.300	5.75	9.60	7.10	135,515	0.25
1.00	0.0	0.350	6.030	10.70	8.00	144,000	0.30
		0.400	6.20	11.10	8.50	144,000	10.0
		10.00	6.20	11.10	8.50		

¹ F-max and Q-max determined from Dutch Cone data.
 1 ft = 0.305 m
 1 in = 25.4 mm
 1 psi = 6.89 kPa
 1 lb = 0.454 kg

Table 6. — F-Z and Q-Z data used in PILGP1 analysis¹
(West Seattle Bridge)

Z (in)	0 depth F (psi)	13 ft depth F (psi)	36 ft depth F (psi)	56 ft depth F (psi)	95 and 98 ft depth F (psi)	Q (lb)	Z (in)
0.0	0.0	0.0	0.0	0.0	0.0	0.0	0.00
0.02	0.0	0.6	1.8	3.3	3.3	66,000	0.020
0.05	0.0	1.6	3.4	5.5	5.5	130,000	0.050
0.10	0.0	3.0	4.8	7.8	7.8	102,000	0.100
0.15	0.0	4.0	5.7	9.8	9.8	200,000	0.150
0.20	0.0	4.8	6.4	11.4	11.4	226,000	0.200
0.25	0.0	5.3	6.82	12.7	12.7	264,000	0.250
0.30	0.0	5.5	7.3	13.5	13.5	284,000	0.300
0.35	0.0	5.5	7.3	14.1	14.1	284,000	0.350
1.0	0.0	5.5	7.3	14.1	14.1		0.420

¹ From measured load transfer data.

1 ft = 0.305 m
1 in = 25.4 mm
1 psi = 6.89 kPa
1 lb = 0.454 kg

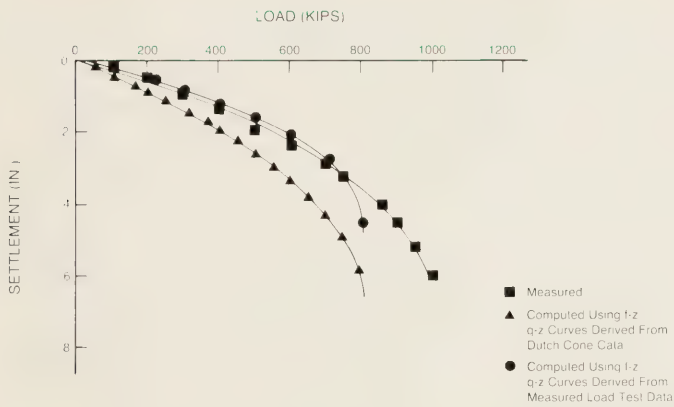


Figure 17. — Comparison between measured and computed load settlement (test pile A, West Seattle Bridge).

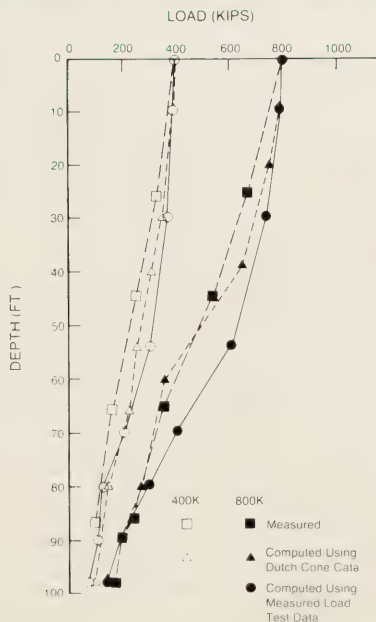


Figure 18. — Comparison between measured and computed load distribution (test pile A, West Seattle Bridge).

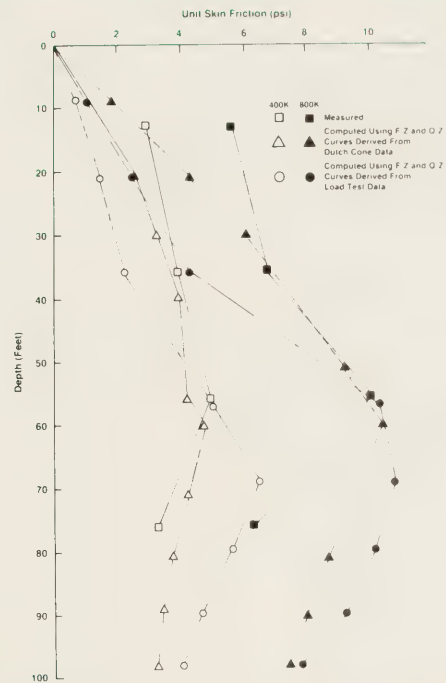


Figure 19. — Comparison between measured and computed unit skin friction (test pile A, West Seattle Bridge).

Pile group instrumentation

Figure 20 shows the pile and soil instrumentation. All piles in the group are instrumented at the top, above the soil line to measure the load transferred from the cap to each pile. Three of the piles, numbered 1, 7, and 10 in figure 20, are instrumented along the entire length with vibrating wire strain gages configured in pairs at each level and with telltale rods as a backup measuring system. These three piles also have pneumatic total pressure cells at the tip. The strain gages were mounted on 5 ft (1.5 m) sections of steel pipe, assembled, and lowered into the pile in the field. The load transferred from the superstructure to the pile cap is measured by four instrumented pipes located in the base of the column. The overall settlement of the pier footing will be measured by first order engineering leveling, and settlement within the soil layers beneath the pier footing will be measured with a five-position mechanical extensometer.

To aid in the interpretation and reduction of the strain gage and telltale readings, a test specimen poured from the same batch of concrete as the foundation piles and instrumented with representative instrumentation is periodically tested to evaluate changes in modulus value caused by concrete creep. Test specimen data will be used to correct pile loads calculated from strain gage and telltale readings.

Long term monitoring

Instrument readings were taken on a monthly basis during construction and at each major construction event. Readings will be taken quarterly for a 5-year postconstruction period. The results of the pile group monitoring program are not yet available.

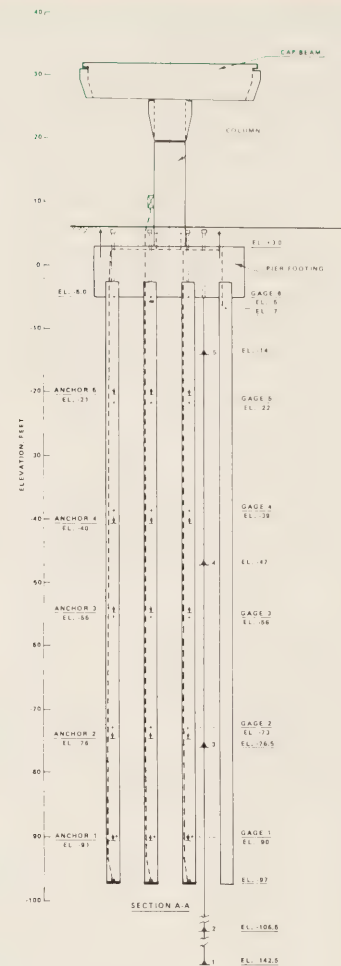


Figure 20.—Pile and soil instrumentation (West Seattle Bridge).

Summary

Natchez Trace Parkway:

- Appreciable soil setup occurred between the initial pile driving and retap of the test pile 7 days later, which points out the need for considering setup when using dynamic measurements for pile capacity predictions.
- Although the pile was designed as an end-bearing pile, approximately 50 percent of the applied load was transferred in side friction, which resulted in the pile reaching the design bearing capacity at a much shallower depth.
- Load distribution changes with construction activity correlated well (qualitatively) with expected behavior.
- The FHWA's PILGP1 method using published criteria correlated well with measured results within the working loads range.

Douge Creek Bridge:

- Significant pore pressures developed during installation of the remaining service piles and falsework piles temporarily reduced load transfer in the instrumented test pile. The magnitude of load change depended on the distance between the test pile and pile driving operations.
- Measured load changes correlated well with construction activities. Good data were obtained on the behavior of a service pile from preconstruction through postconstruction.
- The FHWA's PILGP1 method using Dutch Cone data correlated well with the measured results both within and beyond the working loads range.

West Seattle Bridge:

- The FHWA's PILGP1 method using the Dutch Cone data and the reanalyzed curves from the load test correlated well with measured results.

REFERENCES

- (1) H. B. Ha and M. W. O'Neill, "Field Study of Pile Group Action, Appendix A," Report No. FHWA/RD-81/003, *Federal Highway Administration*, Washington, D.C., March 1981.
- (2) V. N. Vijayvergiya, "Load-Movement Characteristics of Piles," *Proceedings, Ports 1977 ASCE Conference*, Long Beach, Calif., March 1977.

Carl D. Ealy is a geotechnical research engineer in the Construction, Maintenance, and Environmental Design Division, Office of Engineering and Highway Operations Research and Development, FHWA. Mr. Ealy is the principal investigator for the study discussed in this article and for a related study on scale effects between model and prototype pile foundations.

Albert F. DiMillio is a geotechnical research engineer in the Construction, Maintenance, and Environmental Design Division, Office of Engineering and Highway Operations Research and Development, FHWA. Mr. DiMillio is project manager for FCP Project 5P, "Foundations and Earth Structures." Prior to his present position, he served as an area engineer in FHWA's Indiana Division Office and as the Regional Geotechnical Specialist in Region 5, Homewood, Illinois.



Recent Research Reports You Should Know About

The following are brief descriptions of selected reports recently published by the Federal Highway Administration, Offices of Research, Development, and Technology (RD&T). The Office of Engineering and Highway Operations Research and Development (R&D) includes the Structures Division; Pavement Division; Construction, Maintenance, and Environmental Design Division; and the Materials Technology and Chemistry Division. The Office of Safety and Traffic Operations R&D includes the Traffic Systems Division, Safety Design Division, and Safety Research Division. The reports are available from the source noted at the end of each description.

Requests for items available from the RD&T Report Center should be addressed to:

Federal Highway Administration
RD&T Report Center, HRD-11
6300 Georgetown Pike
McLean, Virginia 22101-2296
Telephone: 703-285-2144

When ordering from the National Technical Information Service (NTIS), use PB number and/or the report number with the report title and address requests to:

National Technical Information Service
5285 Port Royal Road
Springfield, Virginia 22161

Loading Spectrum Experienced by Bridge Structures in the United States, Report No. FHWA/RD-85/012

by Structures Division

This report presents the results of a study to determine the loading spectrum experienced by U.S. bridges. More than 27,000 trucks were weighed in seven States using a bridge weigh-in-motion system that uses instrumented highway bridge girders as equivalent static scales to obtain truck gross and axle weights, dimensions, and speed. Because of



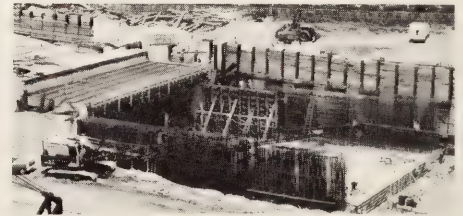
improvements in system software and hardware, weighing can be performed automatically with no traffic observer necessary. The accuracy of the in-motion weighing has been established by repeatability tests and by comparison with static weigh stations.

The report may be purchased from NTIS.

Summary Narrative Report on FHWA Project 5B—Tunneling Technology for Future Highways, Report No. FHWA/RD-85/016

by Structures Division

This report summarizes tunnel research accomplishments including state-of-the-art tunneling techniques developed and proven outside the United States but not yet used in the United States and experimental techniques that have been tried but not yet fully accepted. Specific research studies are discussed dealing with



cut-and-cover tunnels, site investigation, earth movements, environmental criteria, and supporting activities such as research conferences and information exchange. Several appendixes list general references, relevant research, implementation, and supporting activities publications.

The report may be purchased from NTIS.

Limited Sight Distance Warning for Vertical Curves, Report No. FHWA/RD-85/046

by Traffic Systems Division

This report summarizes the procedures and findings of a study of highway signs that warn of restricted sight distance because of crest vertical curves. Driver awareness, understanding, and response to the



existing LIMITED SIGHT DISTANCE (LSD) sign and several alternative signs were measured. The five most promising designs were laboratory tested to assess driver comprehension and assimilation. The two most promising verbal and symbol alternatives were next evaluated in a controlled field study and an observational field study conducted at several vertical curves on two-lane rural roads. The controlled study indicated that both of the alternative signs—one with the legend SLOW HILL BLOCKS VIEW and the other with a symbol in combination with that message—were superior to the LSD sign.

The report may be purchased from NTIS.

Prevention and Control of Highway Tunnel Fires, Report No. FHWA/RD-83/032

by Construction, Maintenance, and Environmental Design Division

This report presents recommendations for reducing the risk, damage, injuries, and fatalities from fires in existing and future highway tunnels. The report is based on an analytical synthesis of tunnel design and operation features that affect fire starts, spreads, detection, damage, control, and related alarm and response systems and procedures. The history of highway tunnel fires; results of controlled tunnel fire experiments; observations of numerous, significant American and foreign tunnels, including those with recent major fires; interviews with tunnel operators; and a risk analysis based largely on truck accidents and fires on all major highways were all considered in the evaluation. Qualitative assessments are made of the effects of traffic, tunnel design, and operations on the risk of fires in highway tunnels. Extensive contributions and reviews were made by fire, highway tunnel, motor carrier, and safety experts.

The report may be purchased from NTIS.



Heavy Vehicle Tests of Tubular Thrie Beam Retrofit Bridge Railing, Report No. FHWA/RD-82/007

by Safety Design Division

This report documents the results of tests with an upgraded passenger vehicle retrofit bridge rail. The previously developed retrofit design was reanalyzed and slightly modified to extend its range of impact performance to include heavy vehicles.

A series of six tests were performed using vehicles ranging from 1,840 lb (0.8 Mg) to 40,000 lb (18.1 Mg). In all tests, the vehicles were successfully redirected, but some resulted in rollover. A modification to the basic structure was introduced, and retests demonstrated that rollover was prevented.

Limited copies of the report are available from the RD&T Report Center.



Implementation/User Items "how-to-do-it"

The following are brief descriptions of selected items that have been completed recently by State and Federal highway units in cooperation with the Office of Implementation, Offices of Research, Development, and Technology (RD&T), Federal Highway Administration. Some items by others are included when they have a special interest to highway agencies.

Requests for items available from the RD&T Report Center should be addressed to:

Federal Highway Administration
RD&T Report Center, HRD-11
6300 Georgetown Pike
McLean, Virginia 22101-2296
Telephone: 703-285-2144

When ordering from the National Technical Information Service (NTIS), use PB number and/or the report number with the report title and address requests to:

National Technical Information Service
5285 Port Royal Road
Springfield, Virginia 22161

Case Studies Using EAROMAR, Report No. FHWA-TS-84-219

by Office of Implementation

To select among alternative pavement investment and maintenance strategies, economic analyses are made to consider both the costs and impacts of each strategy. Such analyses are sensitive to several local factors including initial pavement design and construction, traffic loads, climate, maintenance and rehabilitation policy, maintenance technology, and unit costs.



The report may be purchased from NTIS.

Flexible Delineator Post Test Procedures, Report No. FHWA-TS-84-225

by Office of Implementation

This report provides simplified test procedures to evaluate flexible delineator posts. Many of the variables inherent in previous testing have been eliminated. It is intended that the



simplified procedures can be used to evaluate posts currently installed in a State. The results of the tests then can be correlated with past field performance. Once such correlations have been made, the probable performance of a new post can be determined using data from the series of simplified procedures.

Limited copies of the report are available from the RD&T Report Center.

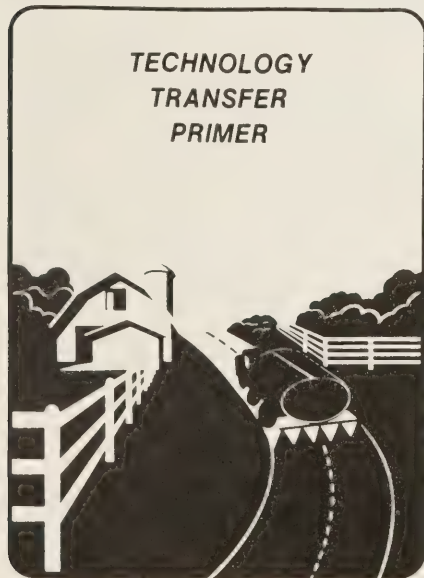
**Technology Transfer Primer,
Report No. FHWA-TS-84-226**

by Office of Implementation

Technology transfer as a working process can have a variety of definitions for different work situations. To be successful the process must be both dynamic and interactive, which emphasizes the human component. Writing, speaking, and visual communication skills are all necessary for effective transfer and dissemination of the information. A prime goal of the process is to have the user accept and adopt the new technology. Obtaining and evaluating feedback on the success of the technology transfer methods used are often an overlooked aspect in the process. All of these factors and others are explored fully in this report.

General information on interpersonal communications and helpful information lists and checksheets for meetings, workshops, conferences, written reports, and newsletter developments are included.

Limited copies of the report are available from the RD&T Report Center.



**Work Zone Accident Data
Process—Training Guide, Report
No. FHWA-IP-85-4**

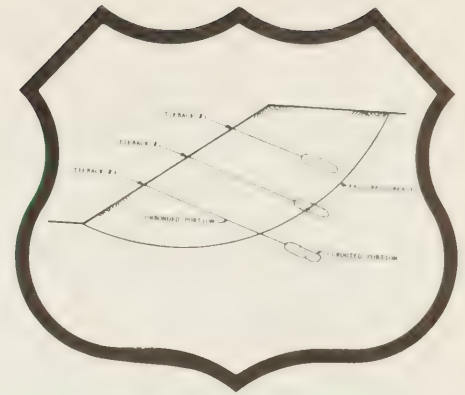
by Office of Implementation

The collection of accident data by law enforcement officials on accidents occurring within construction and maintenance work zones usually is not adequate to assess whether or not the accidents are directly or indirectly related to traffic control or physical roadway features. To determine this relationship, the construction and/or supervisory staff need to collect supplemental data. These



engineers and technicians need to be trained in the techniques of acquiring traffic accident data for immediate assessment of in-place traffic controls and for the Statewide assessment of traffic control standards. This training guide provides the outline, visual aids, and necessary supporting information for a 3- to 4-hour course on the collection of work zone accident data.

Limited copies of the guide are available from the RD&T Report Center.



**Introduction to Slope Stability
Analysis With STABL, Report
No. FHWA-TS-85-212**

by Office of Implementation

STABL, a computer program developed by Purdue University, is a versatile and practical program for State highway agencies to use to analyze slope stability problems for highway slopes. This program can be used to analyze slope failure sections having a circular shape using the simplified Bishop method and also sliding blocks or irregular shapes using the simplified Janbu method. A unique feature of the program allows random surfaces to be generated, allowing the user to more easily determine the critical minimum factor of safety.

This report describes the new version of the program, STABL4. The major enhancement in STABL4 is the addition of the TIEBACK option, which allows the user to specify horizontal or inclined concentrated loads acting on the slope to simulate features such as tiebacks to support excavations or increase slope stability. This option provides a method of analyzing the overall stability of slopes and retaining walls using tiebacks. The program operation has been improved, and a portion of the program dealing with the pseudo static earthquake analysis has been modified.

Copies of the report are available from the RD&T Report Center.

New Research in Progress



The following new research studies reported by FHWA's Offices of Research, Development, and Technology are sponsored in whole or in part with Federal highway funds. For further details on a particular study, please note the kind of study at the end of each description and contact the following: Staff and administrative contract research—*Public Roads* magazine; Highway Planning and Research (HP&R)—performing State highway or transportation department; National Cooperative Highway Research Program (NCHRP)—Program Director, National Cooperative Highway Research Program, Transportation Research Board, 2101 Constitution Avenue, NW., Washington, D.C. 20418.

FCP Category 1—Highway Design and Operation for Safety

FCP Project 1A: Traffic and Safety Control Devices

Title: Improved Signing for Traffic Circles. (FCP No. 41A1074)

Objective: Develop a motorist information system useful for traffic circles of various shapes and designs that will minimize driver confusion by allowing drivers to read and assimilate guidance information before negotiating the circle itself. Determine safety-related surrogate variables for measuring sign-related driver confusion at traffic circles, select signing treatments with the highest potential for reducing driver confusion at traffic circles, and compare the effectiveness of the best alternative sign treatments with standard treatments at selected circles using selected measures of effectiveness.

Performing Organization: New Jersey Department of Transportation, Trenton, N.J. 08625

Expected Completion Date: June 1987

Estimated Cost: \$33,340 (HP&R)

Title: Transport of Hazardous Materials in Arizona. (FCP No. 41A3154)

Objective: Identify operations involving hazardous materials, including radioactive materials and generators of hazardous waste. Conduct surveys to determine volume of flow, kind of material, routes taken, and seasonal variations. Describe, summarize, and display patterns of transportation on computer-based maps. Conduct a risk assessment of transporting hazardous materials. Prepare a final report that presents the findings and discusses their implementation.

Performing Organization: Arizona State University, Tempe, Ariz. 85287

Funding Agency: Arizona Department of Transportation

Expected Completion Date: August 1985

Estimated Cost: \$35,000 (HP&R)

FCP Project 1N: Safety of Nonmotorists

Title: Highway Route Designation Criteria for Bicycle Routes. (FCP No. 31N2032)

Objective: Review highway-bicycle route designation criteria, with the focus on the evaluation/assessment of highway design elements for geometrics, pavements, and roadside development. Include cost, safety, operational, and traffic criteria in the evaluation/assessment. Investigate

State/local liability issues related to specific highway design elements. Prepare a handbook for evaluating roadways for proposed bicycle accommodations.

Performing Organization: The Bicycle Federation, Washington, D.C. 20007

Expected Completion Date: March 1986

Estimated Cost: \$69,140 (FHWA Administrative Contract)

FCP Category 2—Traffic Control and Management

FCP Project 2Q: Urban Network Control

Title: Enhancement of the Value Iteration Program for Actuated Signals. (FCP No. 42Q1222)

Objective: Extend the VIPAS program to include additional left turn geometrics. Collect field data to calibrate, validate, and test VIPAS. Reprogram as necessary to increase the modularization of some of the current subroutines.

Performing Organization: University of Pittsburgh, Pittsburgh, Pa. 15260

Funding Agency: Pennsylvania Department of Transportation

Expected Completion Date: August 1986

Estimated Cost: \$174,985 (HP&R)

FCP Category 4—Pavement Design, Construction, and Management

FCP Project 4B: Design and Rehabilitation of Rigid Pavements

Title: *Methods and Materials for Sealing Concrete Pavement Joints in Utah.* (FCP No. 44B2254)

Objective: Evaluate the short-term performance (3 years) of at least 10 currently available silicone and low-modulus hot pour sealants. Include installation methods and joint configurations.

Performing Organization: Utah Department of Transportation, Salt Lake City, Utah 84119

Expected Completion Date: November 1987

Estimated Cost: \$35,000 (HP&R)

Title: *Methods for Shoulder Joint Sealing.* (FCP No. 34B3445)

Objective: Develop recommendations and criteria for the design, construction, maintenance, and rehabilitation of shoulder joint seals to account for the effects of differential movements between shoulder and pavement and evaluate sealing materials and sealing techniques. Apply the recommendations to the design of new pavements and shoulders and to the maintenance and rehabilitation of existing shoulder joints.

Performing Organization: ERES Consultants, Inc., Champaign, Ill., 61820

Expected Completion Date: November 1986

Estimated Cost: \$135,260 (FHWA Administrative Contract)

FCP Project 4C: Design and Rehabilitation of Flexible Pavements

Title: *Structural Value of Asphalt-Treated Permeable Material and Open-Graded Asphalt Concrete.* (FCP No. 44C1183)

Objective: Determine gravel equivalent factors and R-values for asphalt-treated permeable base and open-graded asphalt concrete by dynaflect deflection measurements at various stages of construction of 11 experimental sections in the field. Use cores and briquettes in the laboratory to measure stability, R-value, cohesion, and resilient modulus.

Performing Organization: California Department of Transportation, Sacramento, Calif. 95807

Expected Completion Date: July 1987

Estimated Cost: \$8,000 (HP&R)

FCP Category 5—Structural Design and Hydraulics

FCP Project 5H: Highway Drainage and Flood Protection

Title: *Development of a Pennsylvania Design Storm Atlas.* (FCP No. 45H3782)

Objective: Perform statistical frequency analyses based on a complete data set of hourly and daily rainfall records in Pennsylvania up to 1984 and develop a series of design storm graphs.

Performing Organization: Pennsylvania State University, University Park, Pa. 16802

Funding Agency: Pennsylvania Department of Transportation

Expected Completion Date: May 1986

Estimated Cost: \$44,630 (HP&R)

FCP Project 5K: Bridge Rehabilitation Technology

Title: *Restoration of Strength in Adjacent Prestressed Concrete Box Beams.* (FCP No. 45K3242)

Objective: Develop concepts for repairing and strengthening bridges constructed with adjacent prestressed concrete box girders that have corroded and fractured prestressing strands. Implement in the field the two most promising concepts and perform load tests on the bridges.

Performing Organization: Wiss, Janney, Elstner Associates, Princeton Junction, N.J. 08550

Funding Agency: New Jersey Department of Transportation

Expected Completion Date: October 1986

Estimated Cost: \$21,130 (HP&R)

FCP Category 9—R&D Management and Coordination

Title: *Evaluation of the Utilization of Protocol Converters.* (FCP No. 49ZZ628)

Objective: Evaluate the use of protocol converters to enhance communications between remote microcomputers and host computers.

Performing Organization: Arizona Department of Transportation, Phoenix, Ariz. 85007

Expected Completion Date: November 1985

Estimated Cost: \$60,000 (HP&R)

RD&T Outstanding Paper Awards Presented

Dr. Yash Paul Virmani, Mr. Thomas J. Pasko, Jr., and Dr. Stephen L. Cohen were the recipients of the 1984 awards in the annual outstanding technical achievement competition held among the employees of the Federal Highway Administration (FHWA) Offices of Research, Development, and Technology (RD&T). This award covers the documentation of any technical accomplishment, which may be a publication, technical paper, report, or package; an innovative engineering concept; an instrumentation system; test procedure; new specification; mathematical model; or unique computer program. Each eligible candidate is judged on excellence, creativity, and contribution to the highway community, general public, and FHWA.

Dr. Virmani, a research chemist in the Materials Technology and Chemistry Division, Office of Engineering and Highway Operations Research and Development, and Mr. Pasko, Chief of the Materials Technology and Chemistry Division, received awards for their research report "Time-to-Corrosion of Reinforcing Steel in Concrete Slabs, Volume 5." This report, FHWA/RD-83/012, presents the findings of an outdoor exposure study of concrete slabs

containing either epoxy-coated rebars or calcium nitrite as a corrosion-inhibiting protective system. The tests were performed under conditions that simulated those found in typical highway bridge decks, and the results are compared with those obtained on uncoated reinforcing steel.

Dr. Cohen, a mathematician in the Safety Research Division, Office of Safety and Traffic Operations Research and Development, received an award for his research paper "Concurrent Use of MAXBAND and TRANSYT Signal Timing Programs for Arterial Signal Optimization." This paper, which was published by the Transportation Research Board in the Transportation Research Record 906, pp. 81-84, 1983, discusses a feasible way to use the MAXBAND program to develop an initial timing plan for TRANSYT. This initial timing plan includes both cycle length and phase sequence optimization. The timing plans produced by the TRANSYT and MAXBAND programs separately were compared with the combined timing plans by using the NETSIM model. The results indicate that measures of effectiveness are substantially improved with the combined timing plans.

United States Road Symbol Signs

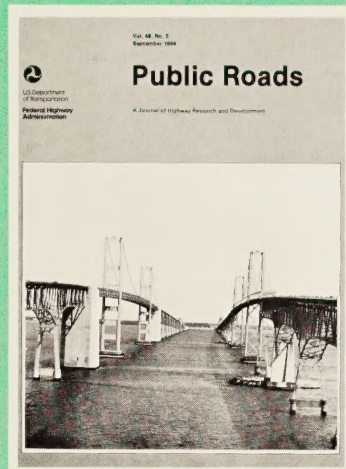
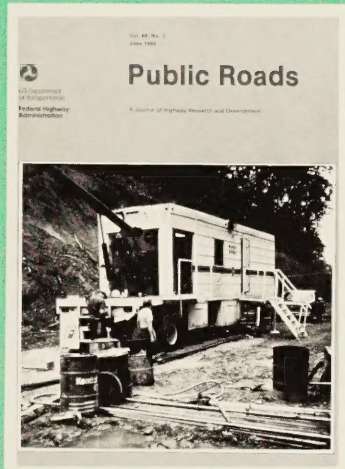
The use of symbols rather than written messages on highway traffic signs in the United States provides instant communication with the driver and overcomes language barriers. The pictorial silhouettes are consistent with those used in many other countries, which is important in view of the growth of international travel. Familiarity with the symbol signs helps Americans traveling abroad as well as

foreign visitors to the United States.

The colors and shapes of road signs used in the United States are shown in this brochure, which may be purchased from the Superintendent of Documents, U.S. Government Printing Office, Washington, D.C. 20402 for \$2.25 (100 copies available for \$50).

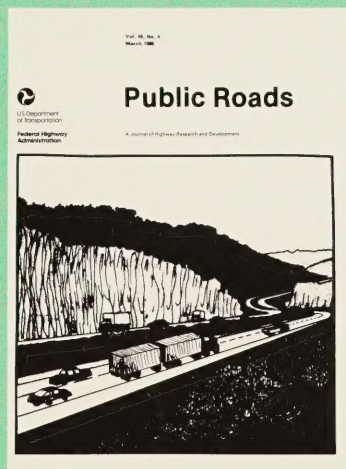
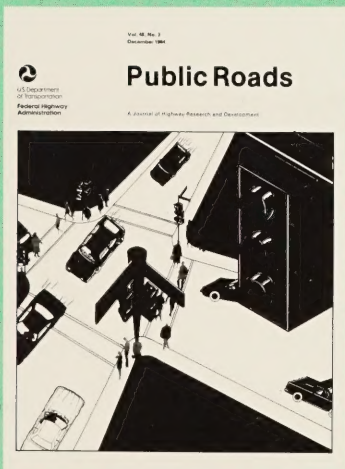


TITLE SHEET, VOLUME 48



Public Roads

A JOURNAL OF
HIGHWAY RESEARCH
AND DEVELOPMENT



VOLUME 48

U.S. Department of Transportation
Federal Highway Administration

June 1984 - March 1985

The title sheet for volume 48, June 1984-March 1985, of *Public Roads, A Journal of Highway Research and Development*, is now available. This sheet contains a chronological list of article titles and an alphabetical list of authors' names. Copies of this title sheet can be obtained by sending a request to *Public Roads*, Federal Highway Administration, HRD-10, 6300 Georgetown Pike, McLean, Virginia 22101-2296.

U.S. Department
of Transportation

**Federal Highway
Administration**

400 Seventh St., S.W.
Washington, D.C. 20590

Official Business
Penalty for Private Use \$300

Postage and Fees Paid
Federal Highway
Administration
DOT 512



SECOND CLASS
USPS 410-210

in this
issue

**The FOIL: A New Outdoor Laboratory
for Evaluating Roadside Safety
Hardware**

**Chemical and Physical
Characterization of Binder Materials**

**Residual Driving Stresses and
Vertically Loaded Piles in Cohesionless
Soils**

**Long Term Monitoring of Pile
Foundations**

Public Roads

A Journal of Highway Research and Development



